MASTER

~~CONFIDENTIAL~~

NYO 9058

C-44a Nuclear Technology - Materials

M3679 24th Ed.

FUEL ELEMENT DEVELOPMENT PROGRAM

FOR THE

PEBBLE BED REACTOR

QUARTERLY PROGRESS REPORT

Feb. 1, 1960 to April 30, 1960

AEC
RESEARCH AND DEVELOPMENT
REPORT

~~CONFIDENTIAL~~

SANDERSON & PORTER

NEW YORK, N.Y.

935-001

LEGAL NOTICE

Printed in USA. Charge $1.65. Available from the U.S. Atomic Energy Commission, Technical Information Service Extension, P. O. Box 1001, Oak Ridge, Tenn. Please direct to the same address inquiries covering the procurement of other classified AEC reports.

DISCLAIMER

NYO-9058
C-44a Nuclear Technology - Materials
M-3679 (24th Ed.)

FUEL ELEMENT DEVELOPMENT PROGRAM

for the

PEBBLE BED REACTOR

QUARTERLY PROGRESS REPORT

February 1 to April 30, 1960

Work Performed Under AEC Contract AT(30-1)-2378

SANDERSON & PORTER
New York, N. Y.

935-002

TABLE OF CONTENTS

Summary

Developments during this quarter have caused a shift in emphasis of the Pebble Bed Reactor Fuel Element Development Program from coatings on the sphere surface to coatings on individual fuel particles as the major deterrent to fission product leakage. In a high level irradiation test, cracks developed in the coatings of specimens coated with pyrolytic carbon and siliconized silicon carbide. In another high level irradiation test, a graphite sphere fueled with Al_2O_3 coated UO_2 particles is showing excellent fission product retention. The leakage factors (i.e. rate of release/rate of production) for long lived volatile fission products such as Kr85m, Kr87, Kr88, Xe133, and Xe135 are ranging from 10^{-9} to 10^{-6}. If this degree of fission product retention is maintained in a large power reactor, it would result in essentially a "clean" primary loop.

A simple crack in a fuel element surface coating will permit the release of all of the volatile fission products in that specimen except those retained by the fuel particles. In view of the failures in surface coated specimens tested to date, it appears to be a difficult task to ensure coating integrity in a large number of specimens because of their low thickness to diameter ratio and exposure to external loads on the fuel element. The test of a single specimen fueled with coated particles takes on added statistical significance, since about 500,000 "fuel elements" are actually being tested.

The acceptability of graphite as a fuel element matrix material was demonstrated when four types of graphite fueled with UO_2 suffered no significant deterioration in structural properties after irradiation to about 6000 KWH which is above the present design objective of the 125 eMW Pebble Bed Reactor. Thus, the incorporation of coated fuel particles, having excellent fission product retention, into a graphite sphere, having excellent structural properties, offers a simple rugged fuel element capable of producing high coolant temperatures while retaining most of the fission products. It is this type of fuel element which will receive major emphasis during the remainder of the PBR Fuel Element Development Program.

The study of the preparation of graphite blanket elements loaded with ThO_2 by the thorium nitrate infiltration process was completed. It was found that graphite densities below 1.45 g/cc and more than 5 infiltration steps

were required to achieve the desired ThO_2 loading. A study of the use of natural graphite to produce high density graphite bodies was started. Densities greater than 2.0 g/cc were produced in a single pressing. The design and construction of an in-pile loop to study fission product behaviour in a recycled helium stream was continued during this quarter. Loop operation is scheduled to start during the quarter commencing Aug. 1.

I.0 Introduction

The basic objective of the Pebble Bed Reactor Fuel Element Development Program is to develop and/or evaluate fuel elements which would be suitable for the economic operation of a large scale Pebble Bed Reactor. The characteristics of a reference design fuel element have been based on design studies of a 125 eMW Pebble Bed Reactor Steam Power Plant (1, 2). This reactor is a high temperature, all-ceramic, helium-cooled reactor, consisting of a randomly packed static bed of fueled graphite spheres. Fuel element characteristics have been completely described in the Phase I Report on the PBR Fuel Element Development Program (3) and are summarized below.

1. The fuel element is a 1-1/2 inch diameter sphere of fueled graphite.
2. Fuel loading is 4.75 gms of uranium in the form of either the oxide or the carbide.
3. The maximum power density is 3 KW per sphere. Maximum surface and center temperature are 1800°F and 2100°F respectively. The design burnup is 5500 KWH per sphere which is equivalent to 6 a/o of total uranium or 40,000 MWD/metric ton of uranium.
4. Fission product retention should be such that the external activity level is $<10^{-6}$ of the activity which would result from the complete release of all isotope chains containing volatile fission products.
5. The spheres shall withstand a 2.0 ft-lb impact load and a 500 lb. compressive load.
6. Other pertinent features are that adjacent fuel elements should not self-weld, fuel element coatings should withstand internal pressure buildup of gaseous fission products, and fuel element surfaces should not dust, abrade or erode.

The PBR Fuel Element Development Program has been arranged to evaluate these various characteristics. Figure 1-1 is a schematic outline of the evaluation program. In general, fuel element specimens are subjected to pre-irradiation testing, followed by irradiation tests to measure fission product retention characteristics and/or the effects of irradiation on physical properties. Final steps in the program include high level

capsule irradiation and operation of an in-pile loop to simulate problems in the primary loop of a Pebble Bed Reactor. The test apparatus used in this program has been described in reference (3). All phases of the evaluation program up to and including the capsule irradiations are being conducted at the Battelle Memorial Institute. The in-pile loop program is being conducted by the Nuclear Science and Engineering Corporation.

The present report describes the results of the PBR Fuel Element Development Program during the period February through April, 1960 which was the fourth quarter of a two-year program. Previous pertinent reports are the Phase I Report (3) covering the first two quarters and the third quarter report (4).

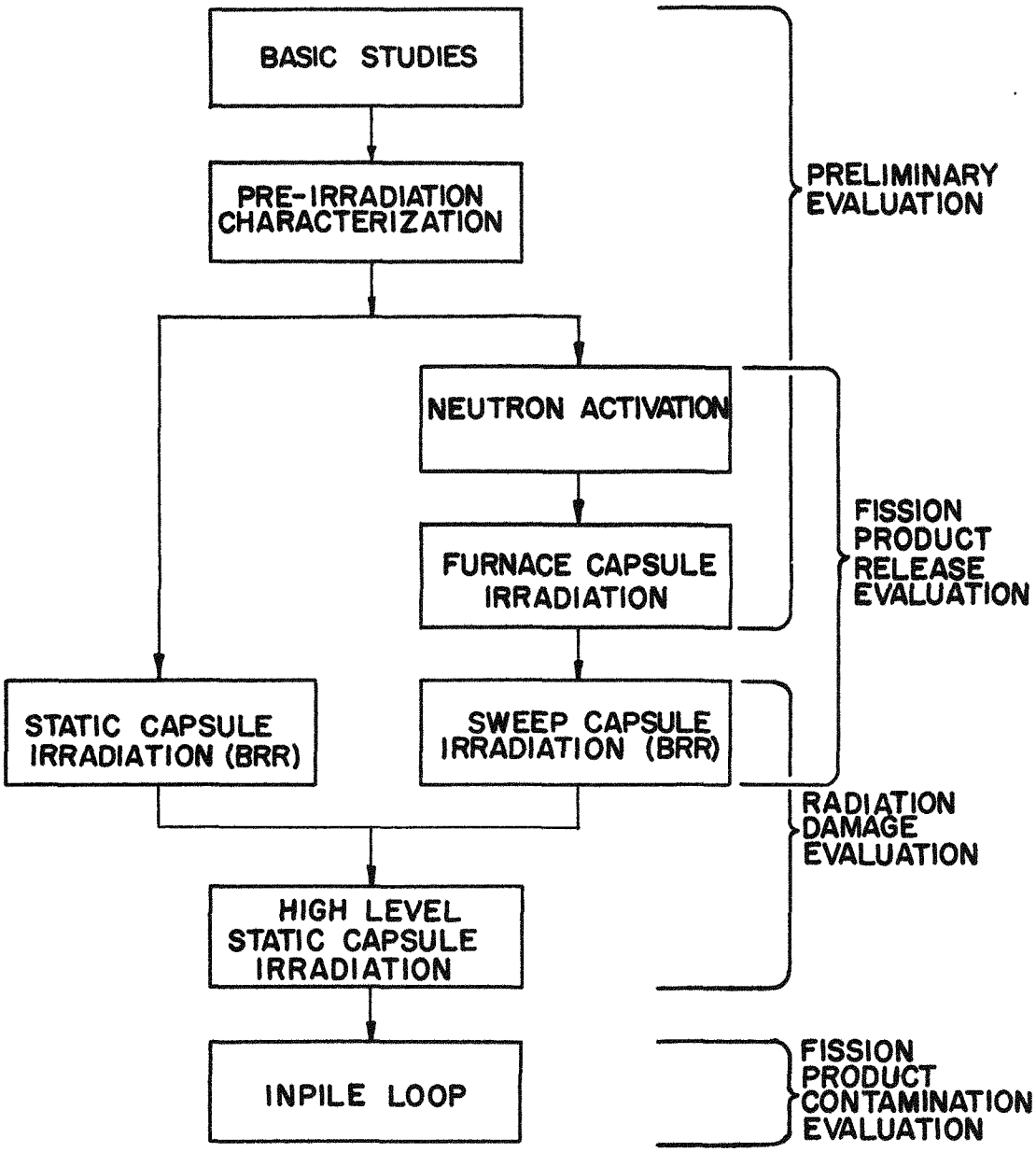

FIG. 1-1 PBR FUEL ELEMENT DEVELOPMENT PROCEDURE

2.0 Materials Development

The majority of the fuel element specimens which have been evaluated in the PBR Fuel Element Development Program have been obtained from manufacturers who have developed various materials which showed some promise of meeting PBR requirements. This procedure has made use of existing developments rather than attempting to duplicate them and it has also given the ultimate suppliers of fuel elements additional experience in producing materials in the form they would eventually be required. Fuel element surface coatings (Section 3.0) are in this category. In other cases, where technology was not already in existence, development programs have been sponsored under the PBR program, such as the thorium nitrate infiltration work, (Section 2.1), natural graphite development (Section 2.2), and fuel particle coatings (Section 4.0). A basic study on the effects of irradiation on UO_2 fueled graphite was concluded this quarter and is described in Section 2.3.

A description of all fuel elements evaluated during this quarter is given in Table 2-1. The manufacturer and pertinent characteristics of the fuel elements are listed. Each type of specimen has been assigned a type number. Prefixes FA and FI refer to the method of fueling the graphite (i.e. admixture and infiltration, respectively). In the case of unfueled specimens, the prefix FX is used. Numbers are assigned serially within each group, and have no special significance. Occasionally, when it is desired to identify a particular ball within a group, an additional identification number in parentheses will be added to the type number. Throughout this report, specimens are referred to only by type number. Consequently, the specimens have been listed numerically in Table 2-1 to permit rapid identification.

TABLE 2-1

SUMMARY OF FUEL ELEMENT TYPES

	INFILTRATED	UNFUELED	
Number	FI-1	FX-3	FX-5
Mfgr.	Syl.	Ray.	AMP
FUEL			
Loaded As	UNH	—	—
Final Form	UO_2	—	—
Particle Size, μ	1	—	—
MATRIX			
Reimpreg.	no	—	—
Net Density	1.65	—	—
Shell Thick.	0	—	—
Bake Temp, °F	1470	—	—
COATING			
Material	—	Pyro-G	Pyro-C
Thickness	—	.060"	.0005"

Manufacturers

- AMP - American Metal Products
- BMI - Battelle Memorial Institute
- Carbo - Carborundum
- GLC - Great Lakes Carbon
- 3M - Minnesota Mining and Manufacturing
- NC - National Carbon
- Ray - Raytheon
- Syl - Sylvania-Corning Nuclear

	ADMIXTURED									
Number	FA-1	FA-2	FA-8	FA-10	FA-16	FA-19	FA-20	FA-21	FA-22	FA-23
Mfgr.	NC	BMI	Carbo	GLC	3M	NC	NC	Ray	NC/BMI	3M
FUEL										
Loaded As	UO_2	UO_2	UC_2	UO_2	UO_2	UO_2	UO_2	UO_2	UO_2	UO_2
Final Form	UO_2	UO_2	UC_2	UO_2	UC	UC_2	UC_2	UC_2	UO_2	UC
Particle Size, μ	100/150	67	100/200	350/420	100/200	100/150	100/150	100/150	100/150	100/200
MATRIX										
Reimpreg.	no	no	no	yes	yes	no	no	no	no	yes
Net Density	1.62	1.49	1.63	1.80	1.75	1.65	1.65	1.65	1.57	1.75
Shell Thick	0	0	0	0	.060"	0	0	0	0	.125"
Bake Temp, °F	2560	2000	3600	2000	3600	4800	4800	4800	2300	3600
COATING										
Location	—	—	Surf.	—	Surf.	—	Surf.	Surf.	Part.	Surf.
Material	—	—	SiC-Si	—	SiC-Si	—	Pyro-C	Pyro-G	Al_2O_3	SiC-Si
Thickness	—	—	.030"	—	.003"	—	.002"	.050"	50μ	.003"

2.1 Infiltration Studies

One method of fueling a graphite body is to infiltrate the pores of the graphite body with fuel-bearing solution, dehydrate the body, and bake it to convert the fuel to a stable solid form, deposited in the pores of the graphite. This infiltration procedure has been of interest to the PBR Fuel Element Development Program because of its potential as an economic method of fueling large batches of spheres, particularly when partially decontaminated fuel is used. A number of spheres fueled with approximately 5.4 gms of fully enriched UO_2 (Specimen type FI-1) had previously been prepared for evaluation as core fuel elements, as described in Appendix B of ref (2).

In order to fully utilize the infiltration process in a Pebble Bed Reactor, the process should also be suitable for preparing blanket elements loaded with ThO_2. However, the available pore volume of a graphite sphere limits the amount of fuel which can be added to the sphere by the infiltration process. Previous studies of a blanketed PBR core (1) showed that 30 to 45 gms of ThO_2 per 1 1/2 inch diameter graphite sphere would be required in blanket elements. Consequently, the Speer Carbon Co. undertook a study to establish process conditions for graphite spheres loaded with ThO_2 by infiltration with thorium nitrate and also to determine the amount of ThO_2 which can be added to graphite as a function of graphite density.

Work on this program was completed during this quarter and a topical report on the infiltration work will be issued during the next quarter as ref (5). The highlights of the results obtained to date are summarized below.

2.1.1 The Infiltration Process

Six sets of 1 1/2 inch graphite spheres having nominal densities of 1.25, 1.35, 1.45, 1.55, 1.65, and 1.75 g/cc were machined from extruded blocks of Moderator Grade B graphite (Speer Carbon Co.) for use in the program. A summary of the mercury porisimetry data on these spheres is given in Table 2-2.

TABLE 2-2

DENSITIES AND POROSITIES OF GRAPHITE SPHERES

Nominal Density, g/cc	Avg. Apparent Density, g/cc	Avg. Pore Volumes, cc/g			
		Total	D> 100μ	100μ <D> .06μ	D <.06μ
1.25	1.240	0.364	0.009	0.305	0.050
1.35	1.339	0.305	0.007	0.250	0.048
1.45	1.421	0.263	0.015	0.200	0.048
1.55	1.579	0.192	0.014	0.118	0.060
1.65	1.666	0.159	0.013	0.110	0.036
1.75	1.732	0.136	0.009	0.074	0.052

After experimenting with several variables, the following standard procedure was adopted for loading the spheres.

1. 3 to 4 spheres of a particular group were outgassed for 15 hrs to a pressure of 5-15 microns of mercury.

2. A water solution containing 76 w/o Th $(NO_3)_4 \cdot 4H_2O$ was prepared. This solution was nearly saturated at the infiltration temperature of 25°C.

3. The outgassed spheres were then flooded under vacuum for 30 minutes with the thorium nitrate solution.

4. Atmospheric pressure was applied to flooded spheres for an additional 15 min.

5. The spheres were removed from the solution, wiped clean of solution, and stored at ambient temperature for 16 hours.

6. The spheres were placed in a vycor tube and heated in a flowing argon stream in accordance with the following schedule:
   a. Temperature raised to 160°C in 30 min and held for 3 hrs to remove water.
   b. Temperature raised to 700°C in 1 hr and held for 3 hrs to decompose thorium nitrate to thorium oxide.

7. Where additional ThO_2 loading was required, the above procedure was repeated.

A number of variations in this process were tried. When a 100°C solution containing 85 w/o $Th(NO_3)_4 \cdot 4H_2O$ was tried, a slight increase in ThO_2 loading per infiltration was found but was not felt sufficient to warrant the complications of providing heated production apparatus. When the vacuum pretreatment was omitted, there was a significant decrease in ThO_2 loading. When longer infiltration times were used, there was no increase in ThO_2 loading. Other variables which were not found to increase the ThO_2 loading were the use of 10 psig pressure during infiltration, a slower heating rate to 700°C, and the use of 12 psig pressure during firing. Shorter heating times at the final temperature and a higher final temperature (950°C) were also investigated. It was found that standard heating cycle produced complete denitration although some further slight weight losses occurred at the higher temperature due to mechanical losses of ThO_2 and graphite in the further handling.

2.1.2 Results of Infiltration Tests

The primary experimental task was to determine the limits of ThO_2 loading in graphite spheres of various densities. Initial experiments showed that the use of successive infiltrations was the best method of raising the ThO_2 loading. It was found that after eight infiltrations, the spheres still did not appear to be near their saturation points. Consequently, a systematic series of runs were made using eight infiltrations at each of the six densities. The results of these runs are summarized in Fig. 2-1 where the cumulative ThO_2 loading is plotted vs. the number of infiltrations for each of the six density groups. Each data point is the average of three spheres. This data is also shown in Fig. 2-2 where the atom density of thorium is plotted vs. the atom density of carbon. As can be noted in Figure 2-1, loadings of 30 gms of ThO_2 can be achieved only in the lower density graphite and that a minimum of 5 infiltrations would be required.

The uniformity of the ThO_2 dispersion in the graphite spheres was checked by sectioning several spheres and analyzing segments from the center region and the edge region. This was done on a number of spheres which had been infiltrated from 1 to 8 times. The ThO_2 distribution was quite uniform. Loadings in the outer region ranged from 4% to 6% of the loading in the center region, the higher values being associated with the greater number of infiltrations.

From this work it is concluded that graphite bodies can by loaded with ThO_2 by the thorium nitrate infiltration process but that relatively large loadings will require the use of lower density graphite and many infiltration steps.

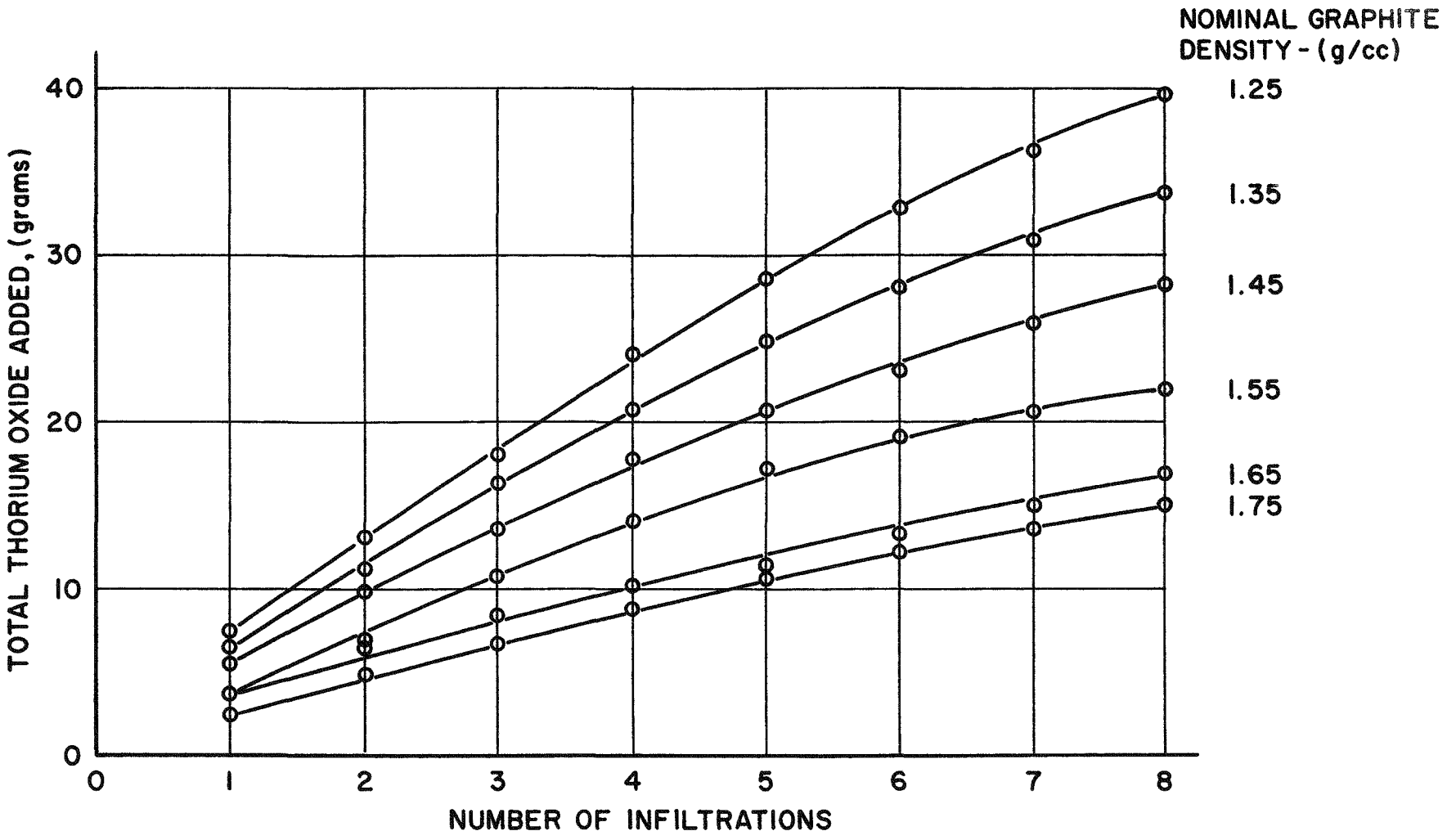

THORIUM OXIDE LOADING vs INFILTRATION FREQUENCY

FIG. 2-1

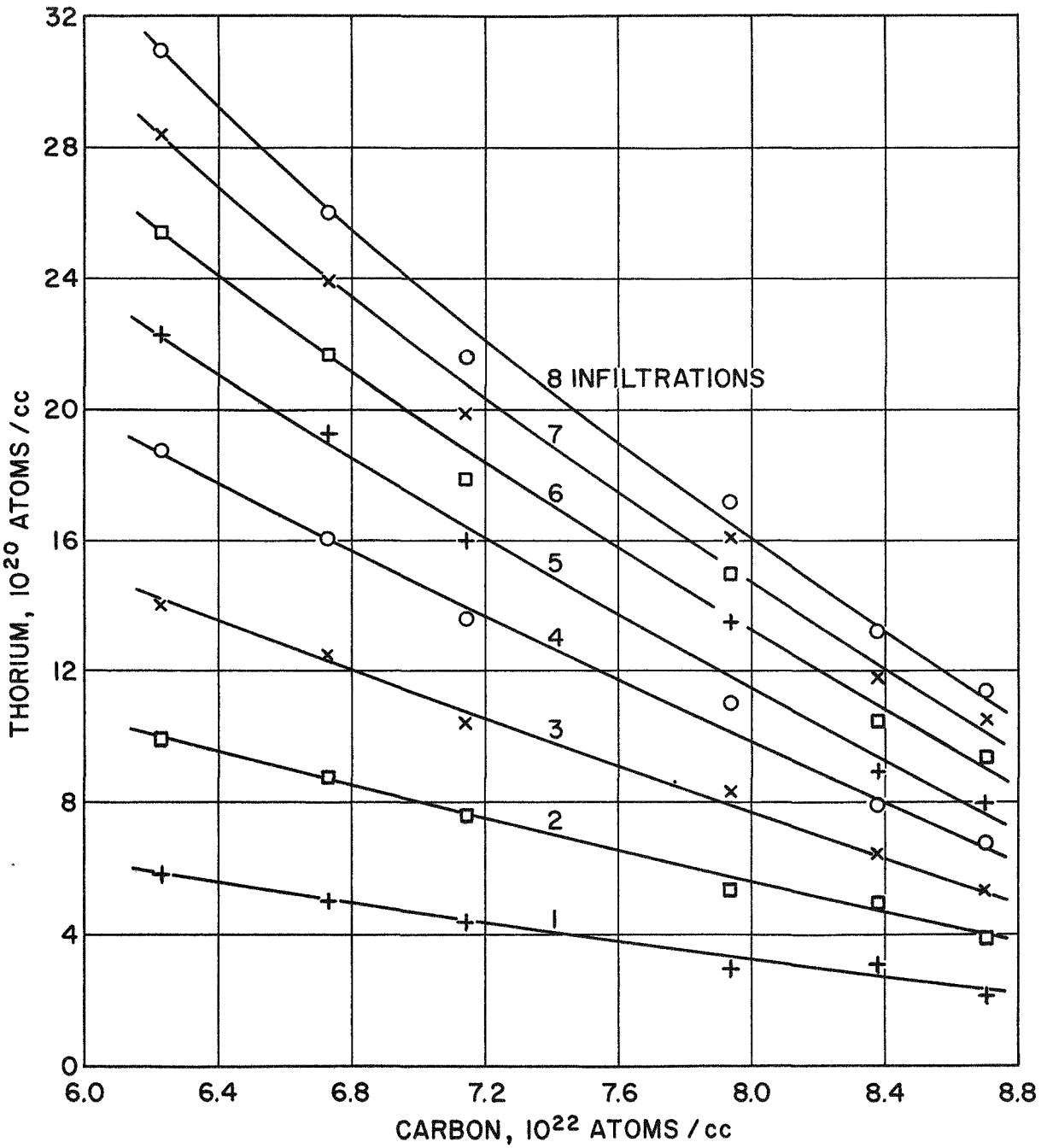

THORIUM AND CARBON DENSITIES
IN INFILTRATED GRAPHITE SPHERES

FIG. 2-2

2.2 Natural Graphite

One inherent characteristic of the Pebble Bed Reactor concept is the fixed 39% voidage in the ball bed region. One method of increasing the amount of carbon moderator in a Pebble Bed core to account for this high voidage is to replace some of the spheres with solid graphite posts. This increases the amount of carbon in the core but at the same time decreases the amount of heat transfer surface in the core. Another method of increasing the amount of carbon moderator is to increase the graphite density of the fueled spheres. For example, in the reference design for the 125 eMW-PBR (2), a graphite density of 1.68 g/cc was used and it was found necessary to replace 25% of the core volume with solid graphite posts to achieve the optimum conditions for that plant. The same effective carbon loading could have been achieved if 2.1 g/cc graphite spheres were used with no fixed graphite posts, thus increasing the thermal capacity by about 33% for the same total core size.

The general method of achieving high density graphite is by successive carbonaceous reimpregnations of the graphite body. Densities up to about 1.9 g/cc have been achieved by this technique. Another method is the use of suitable starting materials which can be molded and baked to directly form a high density graphite body. One such material is natural graphite for which compact densities in excess of 2.0 g/cc have been reported (6).

Because of the potential advantages in using high density graphite, an exploratory program on the fabrication of graphite bodies using natural graphite as a filler material was started at Battelle during this quarter. Although it is possible to compact natural graphite without filler materials to densities in excess of 2.0 g/cc, this type of body would have little strength. Therefore, the major objective of the exploratory program will be to determine the extent to which the density would be lowered by the addition of a binder, in order to achieve an acceptable strength characteristic.

Several types of purified natural graphite were obtained from the Charles Pettinos Graphite Corp. as described in Table 2-3.

TABLE 2-3

NATURAL GRAPHITE MATERIALS

Grade No.	Source	Impurities	Particle size
138	Mexican, amorphous	0.9%	99%, -325 mesh
6353	Madagascar, crystalline	0.1% (B < 1 ppm)	100%, -200 mesh, avg. particle size ~10.6 μ.
6405	Madagascar, crystalline	0.1%	0.03%, +100 mesh 2.03%, -100, +200 mesh 17.98%, -200, +325 mesh 79.96%, -325 mesh.

A trial run consisting of 12 pellets 1/2 in x 1/2 in was made employing both natural and synthetic graphite, and with and without binder. The synthetic graphite was National Carbon Grade 2301 and the binder was a phenolic resin, BV 1600. The pellets were cold pressed under 10,000 psi pressure. The synthetic graphite pellets without binder did not maintain their structural integrity after pressing. After forming, the pellets were cured at 350°F and then baked at 1500°F. The results of this trial run are summarized in Table 2-4.

TABLE 2-4

DENSITIES OF NATURAL GRAPHITE PELLETS

Sample No.	Filler Graphite	Binder Type	Green Density, g/cc	Cured Density, g/cc	Baked Density, g/cc
1	6353	None	2.06	1.98	1.97
2	6353	None	2.19	2.10	2.09
3	6353	None	2.15	2.06	1.95
4	6353	BV1600	1.88	1.90	1.83
5	6353	BV1600	1.93	1.93	1.71
6	6353	BV1600	1.95	1.88	1.73
7	2301	BV1600	1.89	1.57	1.53
8	2301	BV1600	1.78	1.53	1.45
9	2301	BV1600	1.77	1.57	1.49

The resin-bonded pellets exhibited a weight loss due to devolatilization of the organic material while no weight loss was observed on the unbonded natural graphite pellets. Some dimensional shrinkage was observed on all resin-bonded pellets whereas the unbonded natural graphite pellets expanded. As can be noted, the densities achieved using the natural graphite were significantly higher than with the synthetic graphite.

The first attempts to mold 1 1/2 in spheres with the 6353 graphite and no binder were not successful. Some flashback after molding was found, probably due to entrained air on the graphite powder. In one case, the sphere broke into two halves along the equatorial plane upon removal from the die.

In the next attempts, 6405 graphite was used with 16 w/o BV1600 resin binder. The binder was first dissolved in alcohol to enhance wetting and coating of the graphite particles with the binder. A number of spheres were pressed at 10,000 psi. All spheres appeared sound after pressing. No strength measurements on these spheres or on the trial pellets were conducted this quarter.

The preliminary investigation will be completed early during the next quarter. The molded spheres will be subjected to baking and to hot pressing to determine the effect on density. A large number of pellets will be made employing the three natural graphites, several types of binders, and several proportions of binder to filler. Density and compressive strength measurements will be made on these pellets. From this series, it is expected that a region of interest for further investigation will be found.

2.3 Uncoated Specimens Fueled with UO_2

In selecting the fissile material compound in a uranium-graphite fuel element, the oxide form has a number of advantages over the carbide form, such as ease in handling during fabrication and ease of reprocessing. The greatest limitation on UO_2 is its reaction with the graphite matrix at high temperatures. Evidence of reaction at temperatures as low as 2400°F have been reported (7), however stability during the short baking time at 2560°F during fabrication is excellent. By dispersing fissile material throughout the graphite moderator, the Pebble Bed Reactor offers the best opportunity of producing high coolant outlet temperatures (1200 to 1400°F) while keeping peak fuel temperatures below 2100°F and thus UO_2 can be considered for PBR applications.

A capsule irradiation experiment was performed in an attempt to determine whether radiation would affect the reaction between UO_2 and graphite at temperatures approaching 2100°F. Another objective of this experiment was to assess the effect of high temperature irradiation on the strength and dimensional changes of fueled graphite. Four types of uncoated graphite spheres each fueled with a different type of UO_2 were tested. The specimen designations and the UO_2 particle sizes were: FI-1 (1 μ UO_2), FA-2 (67μ UO_2), FA-1 (100μ) and FA-10 (400μ). A further description of these types is included in Table 2-1 and ref. (3). The specimens were irradiated in Static Capsule SP-4. The design and operation of this capsule is described in Section 5-1. The exposure conditions for the specimens are summarized in Table 2-5, where the burnup has been calculated from the thermal data and the irradiation time.

TABLE 2-5

EXPOSURE CONDITIONS FOR UO_2 FUELED SPECIMENS IN CAPSULE SP-4

Specimen Type	Measured Graphite Block Temp, °F	Ht. Gen., Rate, KW	Calculated Surface Temp, °F	Central Temp, °F	Burnup (b) KWH/Ball
FI-1(E8)	1400	2.3	1750	1850	7700
FA-2(E8)	1400	2.2	1750	1900	7400
FA-1(E82)	1300	1.9	1600	1750(a)	6400
FA-10(E5)	1300	1.7	1600	1700	5700

(a) Measured temperature. One thermocouple was imbedded in the center of this specimen. All other control temperatures were calculated.

(b) For PBR specimens, 1 KWH is equivalent to 7.2 MWD/metric ton of U, 4.4×10^{15} fissions/cc of specimen, or .0011% of the U235 atoms fissioned.

During the course of the SP-4 irradiations, there were the usual variations in the specimen operating conditions due to shifts in flux patterns, scrams, etc. The values listed in Table 2-5 are typical average values for the irradiation period. The maximum and minimum recorded temperatures in the center of the FA-1 specimen were 2070°F and 1510°F respectively. The fluctuations in the temperature difference between the measured central temperature and the measured block temperature of the FA-1 specimen was too great to permit a statement that this temperature difference increased with irradiation because of deterioration of thermal conductivity of the graphite.

In parallel with the irradiation of Capsule SP-4, four specimens identical with those in the capsule were heated in an out-of-pile furnace, duplicating the time-temperature pattern of the irradiated specimens. This step was taken in order to distinguish between radiation and temperature effects.

Special flats, approximately 1/2 inch in diameter, were machined and polished on all specimens so that "before and after" photomicrographs could be taken of specific fuel particles. These pictures are all shown in Figures 2-3(a-d) through 2-6(a-d). The a and b photos were taken before and after the out-of-pile heating test while the c and d photos were taken before and after the irradiation tests. Scribe marks were made in the graphite around selected fuel particles to permit their identification after testing.

Figures 2-3a through 2-3d are of the infiltrated specimen. The fuel particles, believed to be of the order of 1μ in size, are indistinguishable in all of the views. One grey particle, approximately 10μ in size can be noted in Figure 2-3c but appears to be missing after irradiation (Figure 2-3d). Figures 2-4a through 2-4d are of the FA-2 specimens. No clearly discernable fuel particles can be detected in the out-of-pile specimen, however, a fuel particle is clearly noted in the irradiated specimen. The particle size appears unaffected by irradiation and the characteristic appearance of uranium carbide is not evident.

Excellent views of the fuel particles in the FA-1 specimens were obtained as noted in Figures 2-5a through 2-5d. No change in particle dimension or appearance can be noted in the out-of-pile test. Although there is no apparent carbide formation in the in-pile test there is a noticeable increase in the void region around the particle (Fig. 2-5d). The increase in "inner radius" of the graphite void is approximately 20μ. Since fission fragment

Out-of-Pile Heating Test of Infiltrated Graphite
Specimen Type FI-1

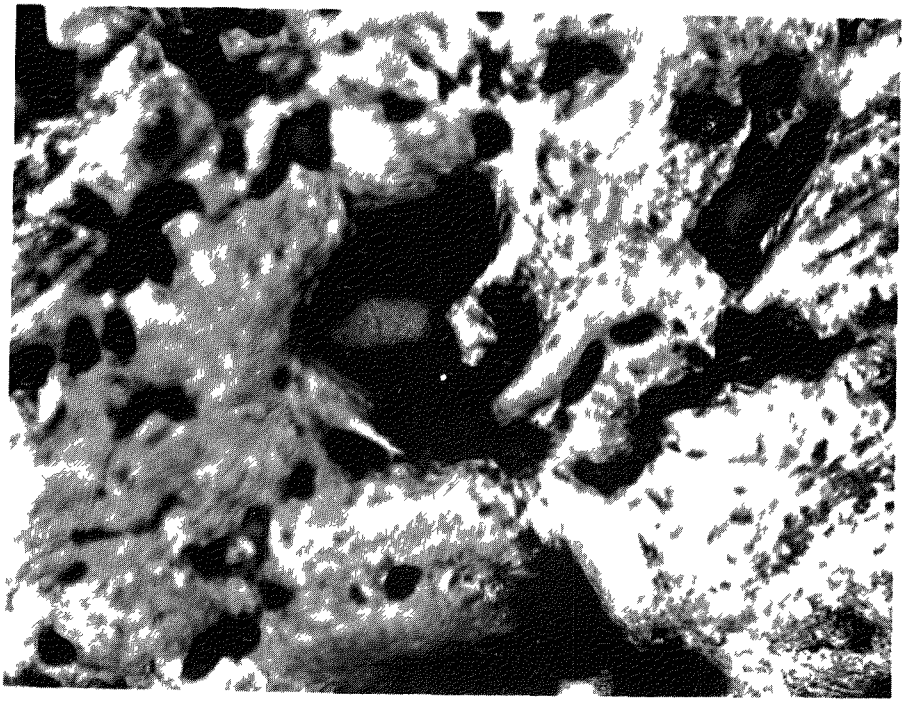

Fig. 2-3a. Before heating, 250x

Fig. 2-3b. After heating, 250x

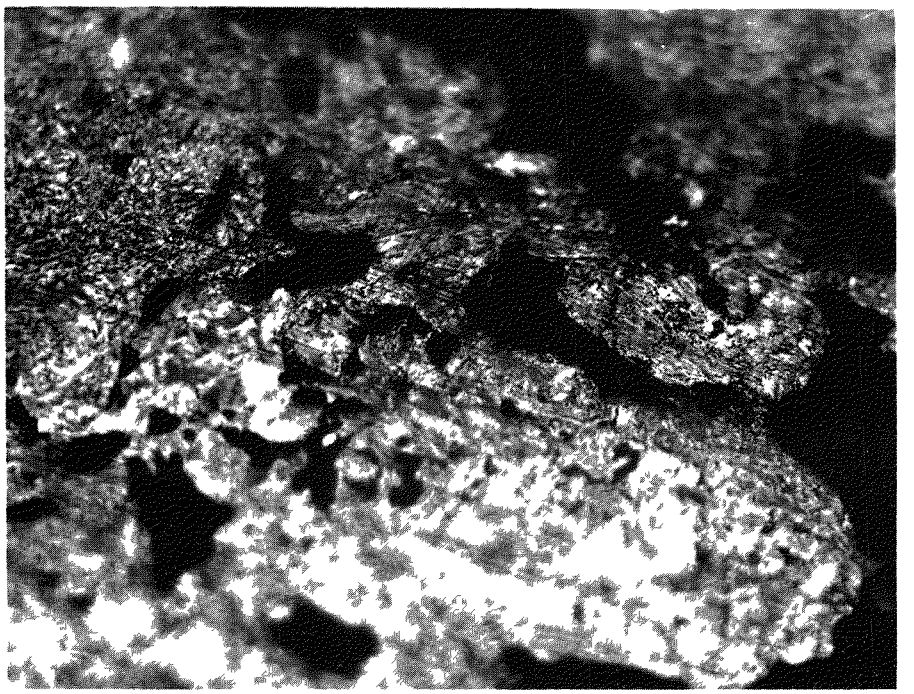

Fig. 2-3c. Before irradiation, 250X.

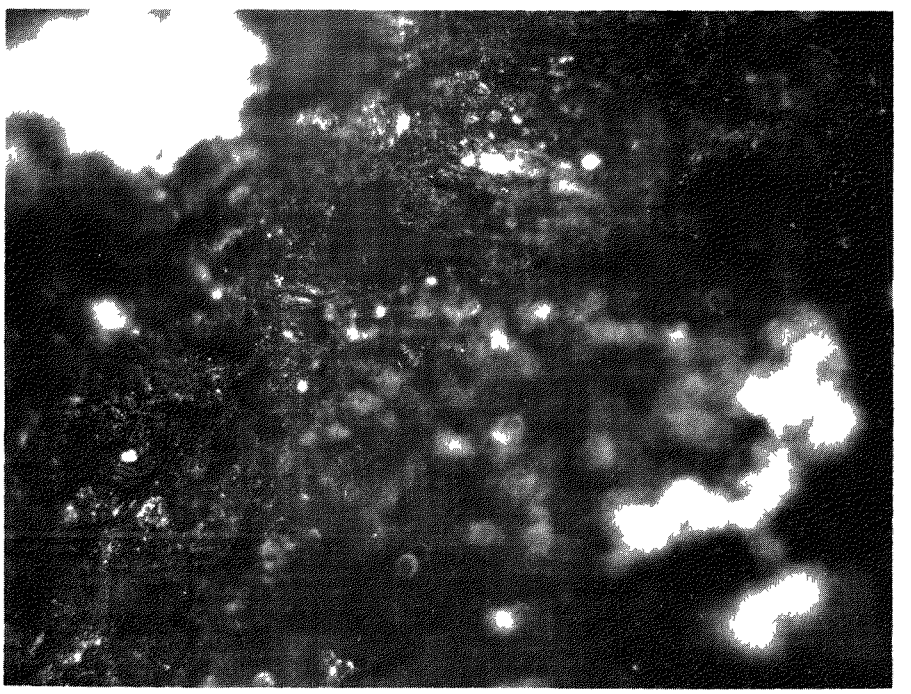

Fig. 2-3d. After irradiation, 250X.

Out-of-Pile Heating Test of 67μ UO_2 in Graphite
Specimen Type FA-2

Fig. 2-4a. Before heating, 250x

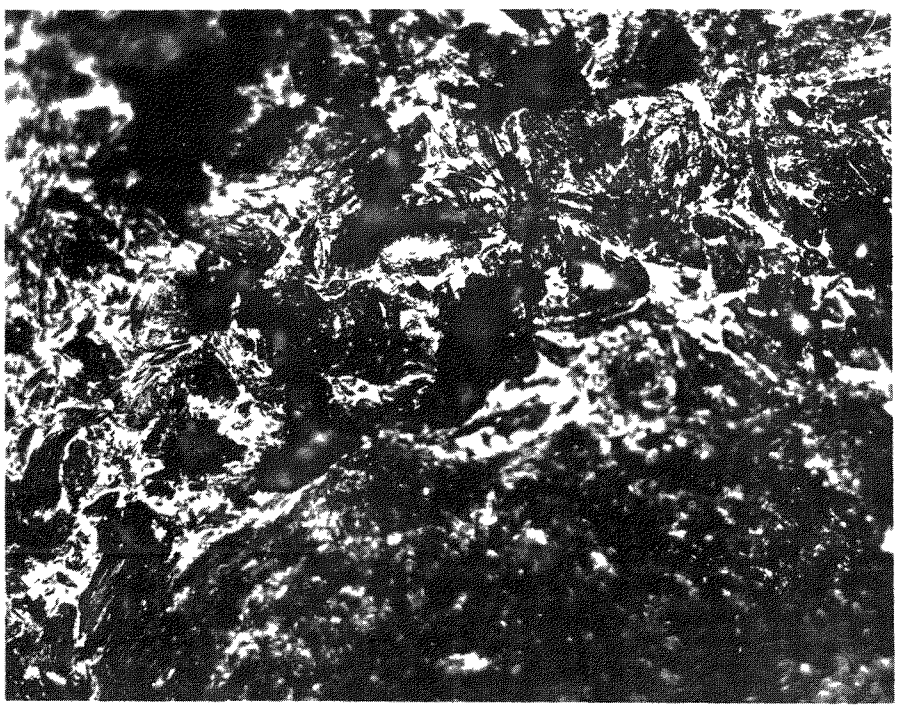

Fig. 2-4b. After heating, 250x

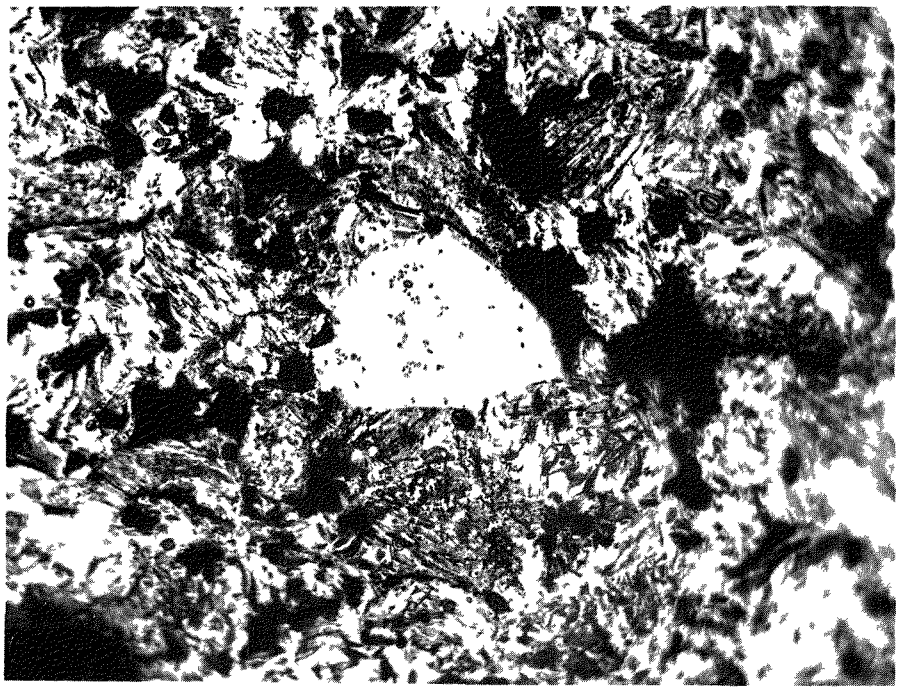

Fig. 2-4c. Before irradiation, 250X.

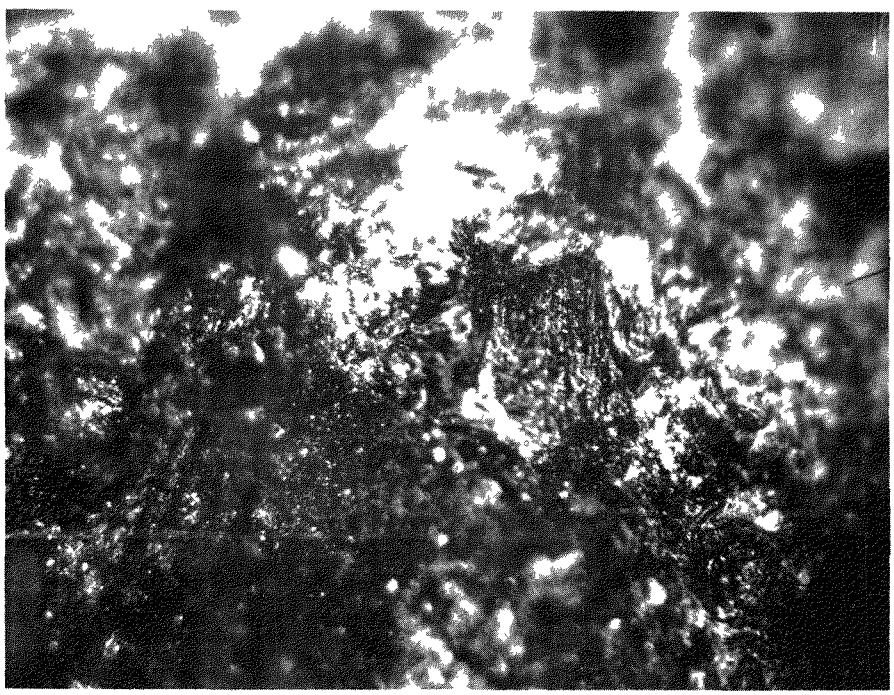

Fig. 2-4d. After irradiation, 250X.

Out-of-Pile Heating Test of 105/149μ UO_2 in Graphite
Specimen Type FA-1

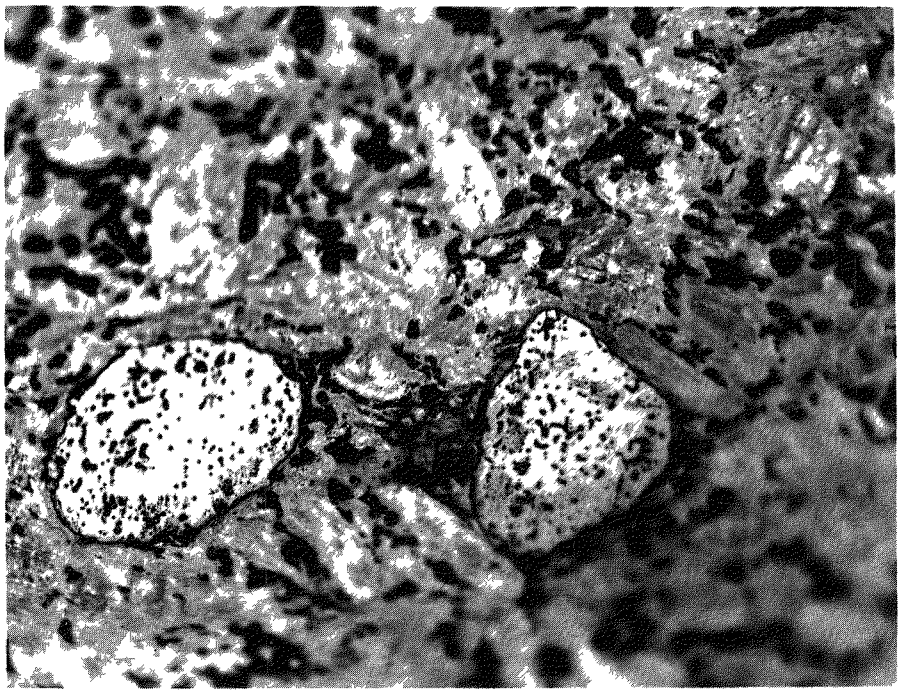

Fig. 2-5a. Before heating, 250X.

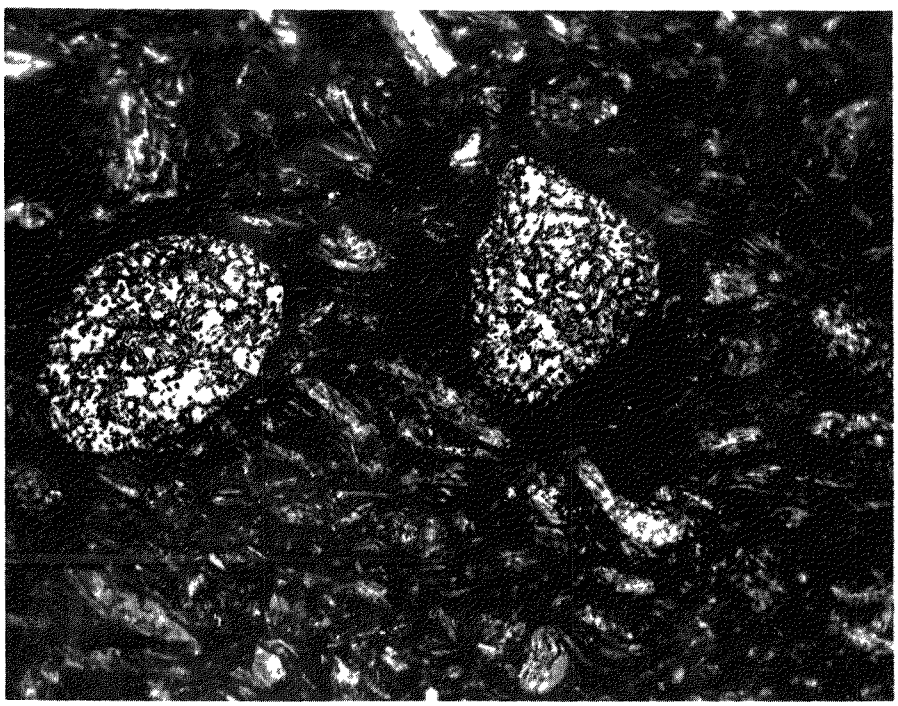

Fig. 2-5b. After heating, 250x

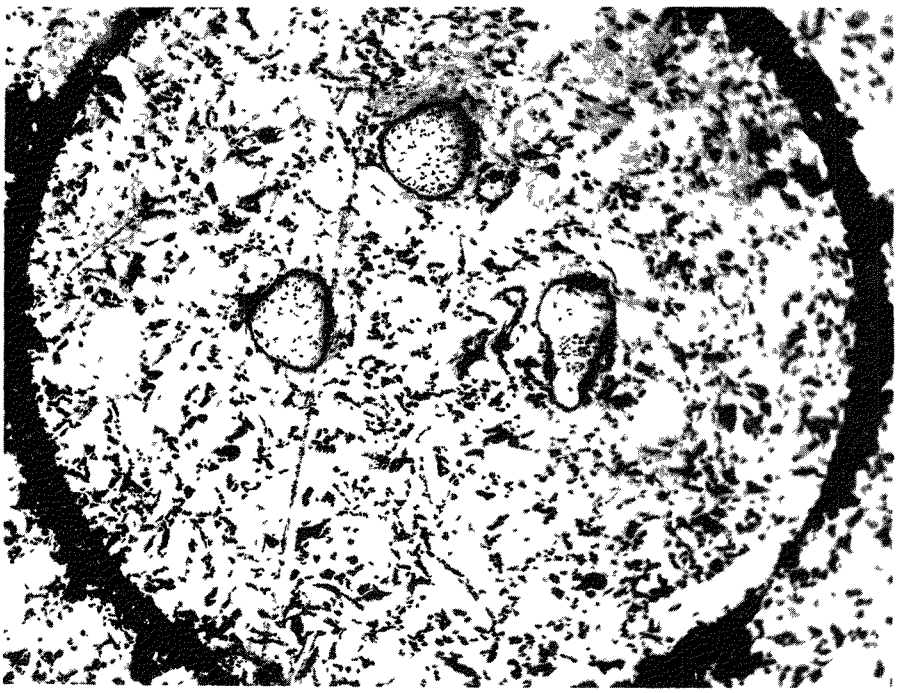

Fig. 2-5c. Before irradiation, 100X.

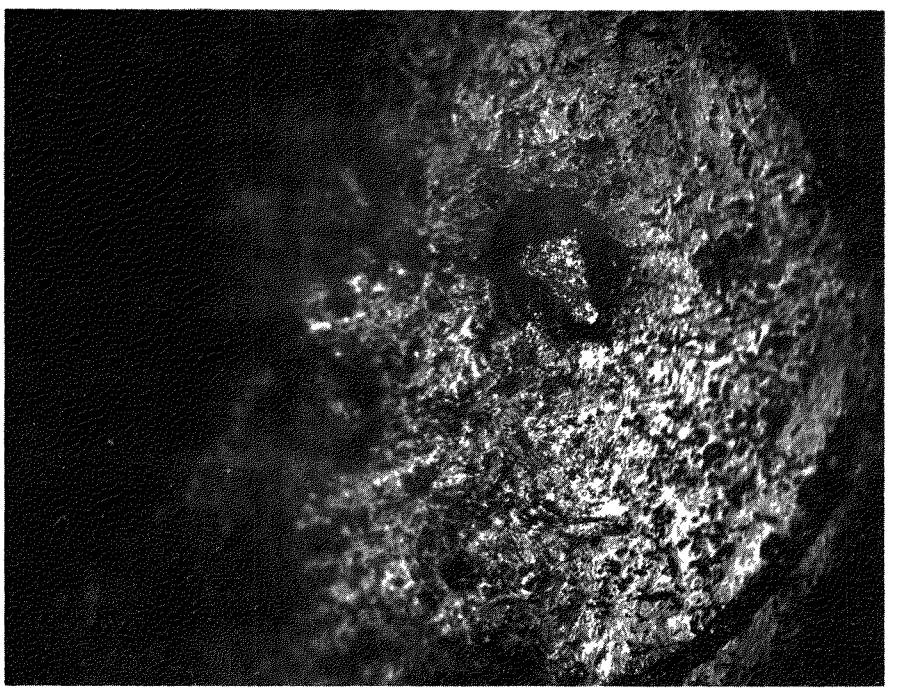

Fig. 2-5d. After irradiation, 100X. Note void space around UO_2 particles.

Out-of-Pile Test of 350/420μ UO_2 in Graphite
Specimen Type FA-10

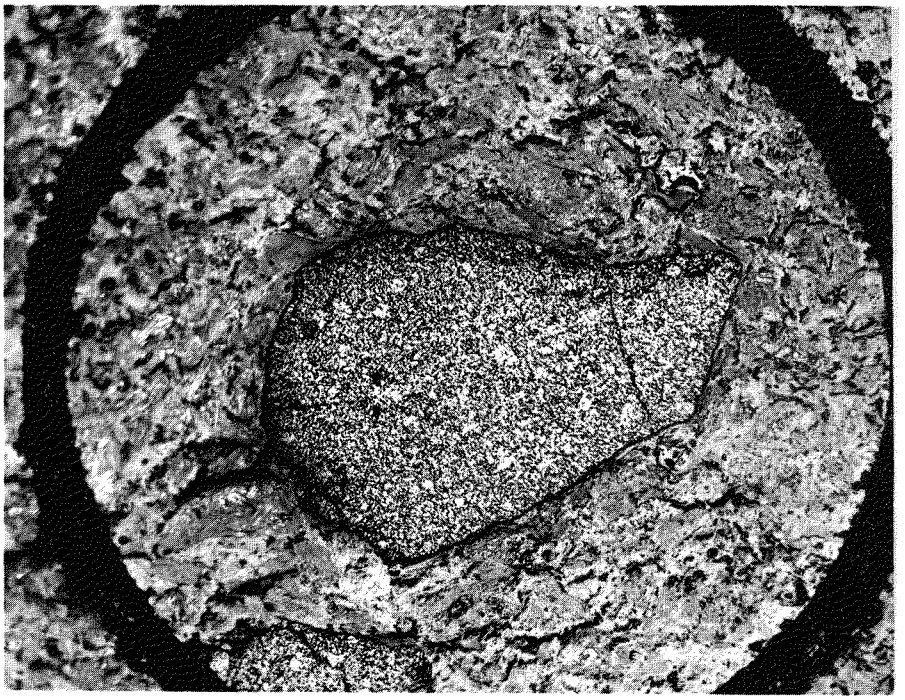

Fig. 2-6a. Before heating, 100X.

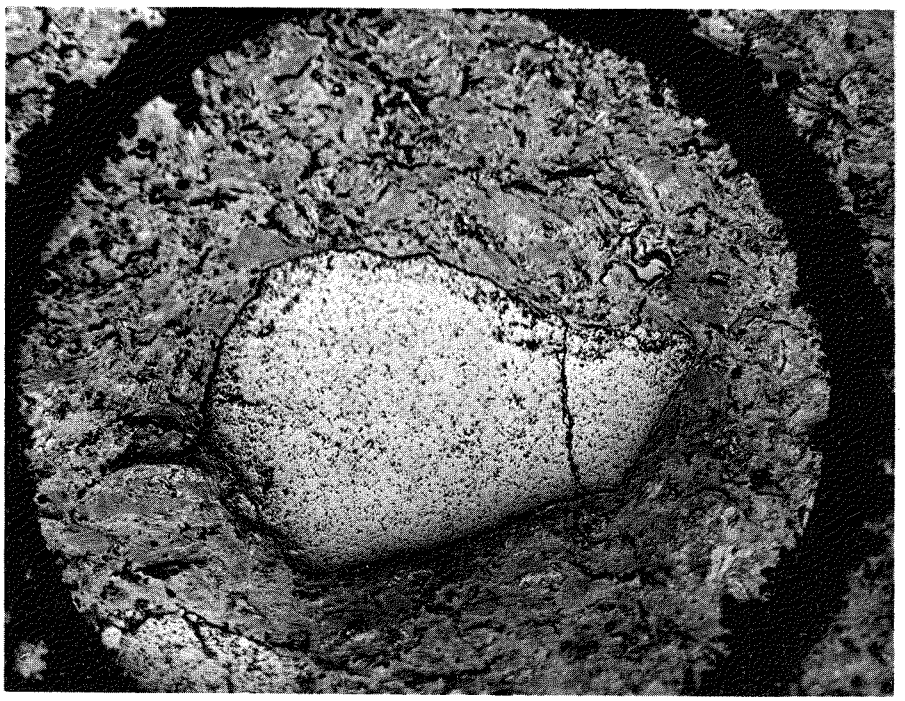

Fig. 2-6b. After heating, 100X.

In-Pile Test of 350/420μ UO_2 in Graphite
Specimen Type FA-10

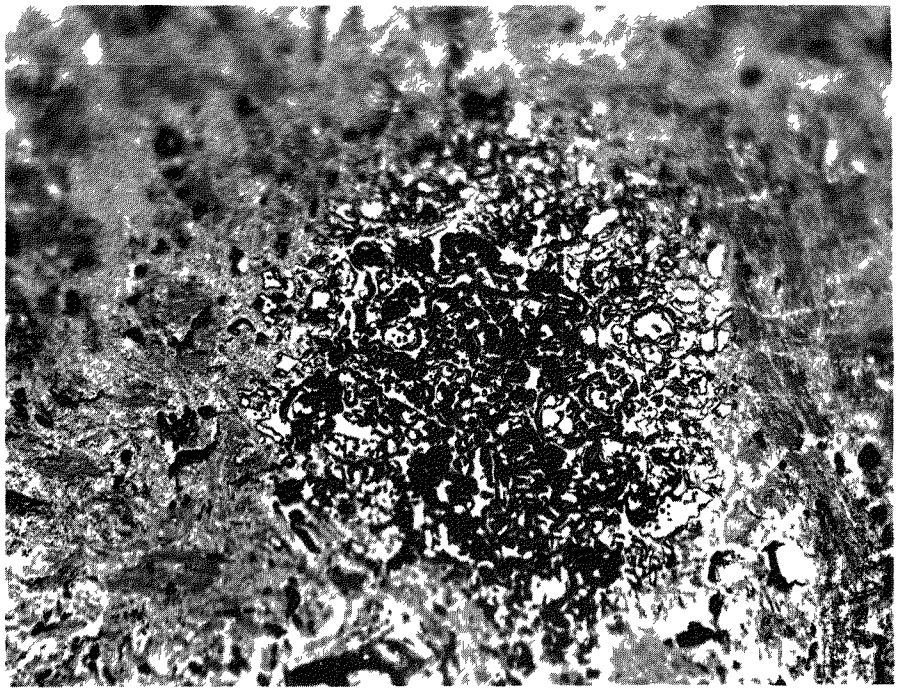

Fig. 2-6c. Before irradiation, 250X.

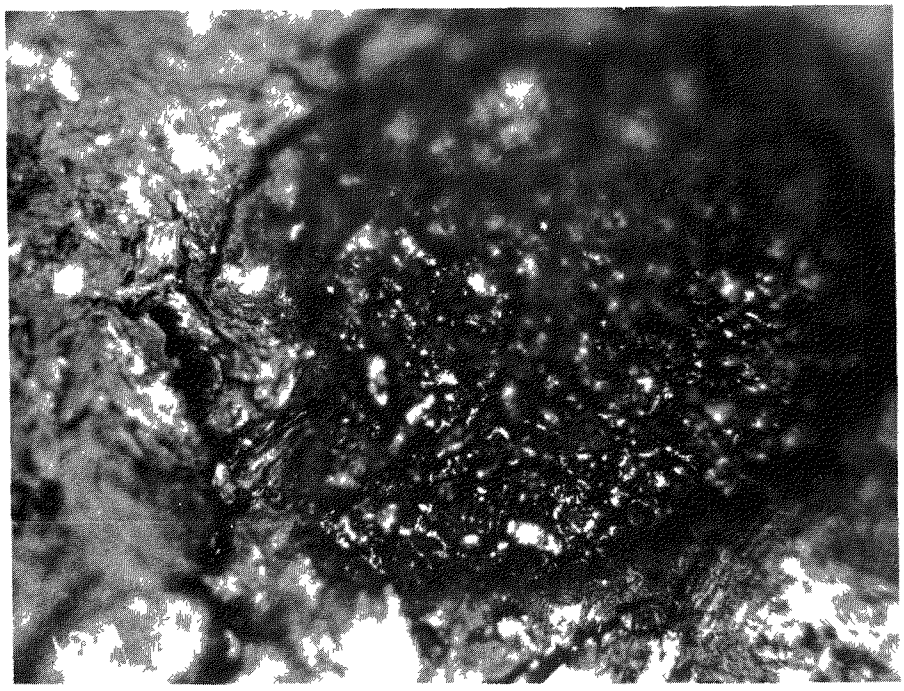

Fig. 2-6d. After irradiation, 250X.

recoil range in graphite is also about 20μ, this result strongly suggests that the local graphite region directly affected by fission fragment recoils have become hardened and brittle and most probably came out during polishing of the specimen. Deterioration of the fuel particle itself is also noted, the decrease in "radius" being about 10 microns. Figures 2-6a through 2-6d are of the FA-10 specimens. No affect on the UO_2 particles can be noted in the out-of-pile test. Although the original fuel particle in the irradiation test appears badly fragmented, no significant affect to the particle or the graphite matrix can be noted in the post-irradiation view.

Other measurements made on the in-pile and out-of-pile specimens were macroscopic examination, weight change, dimensional change, and impact strength. The weights and dimensions of all specimens prior to testing are given in Table 2-6.

These specimens had additional flats machined on their surfaces to permit accurate measurement of their diameters. The dimensional shrinkages noted in Table 2-6 are predominantly due to irradiation effects since insignificant shrinkages were found for the out-of-pile specimens except in the case of the FI-1 type. The irradiation-induced shrinkages do not decrease with increasing UO_2 particle size (i.e. decreasing recoil fission fragment exposure to the matrix)as might be expected which implies that properties of the graphite matrix and/or neutron damage are the significant factors rather than damage by fission fragment recoil. The FI-1 specimen has a fully graphitized matrix (Type AGOT). The low shrinkage of the FA-2 specimen could be related to the low degree of graphitization and low density (1.50 g/cc) of this specimen which was made with a coke filler and baked at only 2000°F. Both the FA-1 specimen and the FA-10 specimen have a graphite filler but the pitch binders were not graphitized, again due to the relatively low bake temperature. The FA-10 specimen was re-impregnated several times to raise its graphite density to 1.80 gm/cc. The graphite density for the FA-1 specimen was 1.62 gm/cc. It would appear that the high shrinkage of the FA-10 specimen, in spite of the minimum fission fragment exposure due to its large 400 μ fuel particles, is associated with its large number of reimpregnations.

Identical specimens from the same production batches as the FA-1 and FI-1 type had also been irradiated in a previous capsule, SP-1. This irradiation was described in ref (2). The dimensional changes from Capsule SP-1 are compared with those observed in Capsule SP-4 in Table 2-7. The infiltrated specimen (FI-1) showed a smaller shrinkage at the longer exposure which indicates that the lower temperature of the SP-1

TABLE 2-6

WEIGHTS AND DIMENSIONS OF UNCOATED UO_2 FUEL SPECIMENS IN OUT-OF-PILE AND IN-PILE TESTS

Specimen Type and No.	Test	Weight Change		Dimensional Change			
				Polar (a)		Equatorial (b)	
		Initial, gms.	Change, %	Initial, in.	Change, %	Initial, in.	Change, %
FI-1(E8)	In-Pile	52.3128	-0.40	1.477	-0.76	1.476	-0.67
FA-2(E8)	"	45.1378	-0.55	1.447	-0.03	1.452	-0.08
FA-1(E82)	"	51.8004	-0.11	1.478	-0.47	1.490	-0.52
FA-10(E5)	"	56.0927	-0.06	1.469	-0.69	1.469	-0.81
FI-1(E2)	Out-of-Pile	52.621	-0.77	1.487	-0.07	1.479	-0.10
FA-2(E7)	"	45.351	-2.55	1.447	0.0	1.449	-0.07
FA-1(E76)	"	51.892	-0.45	1.476	0.0	1.476	0.0
FA-10(E6)	"	55.727	-0.09	1.474	0.0	1.471	0.0

(a) Molding or extrusion axis

(b) Perpendicular to molding or extrusion axis

irradiation may have been the dominant factor. This effect is not borne out in the case of the admixture specimen (FA-1), although the shrinkage increase with the higher temperature irradiation is only 50% of the exposure increase. Due to the lower fission fragment recoil exposure (i.e. larger fuel particle size) in the admixture specimen, the effect of fast neutron damage could be relatively more significant in the admixture element than in the infiltrated element.

TABLE 2-7

COMPARISON OF DIMENSIONAL CHANGES OBSERVED IN CAPSULES SP-1 AND SP-4 FOR FA-1 AND FI-1 SPECIMENS

	Type FI-1			Type FA-1		
Capsule	Temp. °F	Exposure KWH/Ball	Dimensional Change, %	Temp. °F	Exposure KWH/Ball	Dimensional Change, %
SP-1	1350	1500	-0.93	1350	1400	-0.22
SP-4	1800	7700	-0.71	1700	6400	-0.50

The weight loss data shown in Table 2-6 clearly indicates that temperature effects are most significant since the weight losses are all larger for the out-of-pile specimens. It is interesting to note that the relative order of weight losses are the same for both the out-of-pile and the in-pile specimens. The major factor in these weight losses is probably further devolatilization of adsorbed gases.

Impact tests were performed on these specimens by dropping a steel weight onto the specimen from successively increasing heights to the point of failure. Since previous tests (ref. 2) had shown that PBR specimens actually increase in compressive strength with irradiation, this test was not selected for the SP-4 specimens. The impact test results for the out-of-pile and the in-pile specimens are summarized in Table 2-8. For purposes of comparison, the impact data on as-received specimens, and the admixtured and infiltrated specimens after irradiation in Capsule SP-1 are also included.

Although there is random scatter in this impact data, all values are significantly above the design objective of 2.0 ft. lbs for PBR specimens except the FA-2 type. No significant effect of irradiation on impact strength can be noted, although there is a slight drop in impact strength for several of the specimens.

TABLE 2-8

IMPACT DATA ON UNCOATED SPHERES

Specimen Type	As-Received		After Out-of-Pile Heating		After SP-1 Irradiation		After SP-4 Irradiation	
	Failure, Ft-lbs.	No. Impacts	Failure, Ft-lbs.	No. Impacts	Failure, Ft-lbs.	No. Impacts	Failure, Ft-lbs.	No. Impacts
FI-1	12.5	12	9.4	22	10.4	12	11.7	35
"	11.5	11						
"	13.6	11						
FA-1	11.5	11	6.8	16	8.4	10	9.4	28
"	11.5	11						
"	7.3	5						
FA-2	7.5	15	6.8	16			3	9
FA-10	10.4	10	10.6	23			12.5	37

The Capsule SP-4 irradiation has demonstrated that more than one type of uranium-graphite material has adequate structural properties to meet the reference design conditions of a large Pebble Bed Reactor. Some further work will be required to establish the cause and nature of the weight losses observed, but nonetheless, our initial selection of graphite as a high temperature ceramic structural material for use in PBR fuel elements appears fully justified.

3.0 Surface Coatings

One of the earliest approaches to fission product retention was the application of a ceramic coating to the outside surface of the spherical PBR fuel element. A variety of surface coatings have been investigated in the program (2, 3). Two of the most promising surface coatings received additional evaluation during this quarter. These were a silicon carbide coating bonded with silicon and a pyrolytically deposited carbon coating. The use of surface coatings presents certain problem areas. Impact strengths are significantly reduced due to the thin, hard and less resilient nature of the coating compared with the graphite matrix. However, by proper choice of graphite material and coating thickness, fuel elements meeting the 2.0 ft. -lb. requirement can be made. Also coatings having adequate adherence to the graphite body and sufficient abrasion resistance to withstand the fuel flow pattern through PBR cores have been found. Coating materials which will not self weld and caused the packed bed to freeze up must be avoided. Also, if the coating material reacts with uranium, an unfueled graphite shell must be placed between the fueled graphite core and the coating. These factors, together with the ability of the coating to retain fission products, have formed the basis for the evaulation program.

3.1 Silicon Carbide Coatings

The interest in silicon carbide coatings for Pebble Bed Reactor fuel elements stems from their excellent potential as a barrier to fission product leakage at high temperatures. Actually, this property is due to the presence of a continuous phase of silicon throughout the silicon carbide grains in the coating. This material is referred to as siliconized carbide (Si-SiC). Test results during previous periods had indicated good fission product retention by this material (2). However, due to the potential reaction between free silicon and the fuel particles causing the surface coating to become contaminated with fuel, it has been necessary to include an unfueled graphite shell between the fueled graphite core and the Si-SiC coating. Irradiation of this type of specimen in capsule SP-3 (3) caused the coating adjacent to incipient flaws in the unfueled shell to fail under the effects of an internal temperature gradient. Another problem area is the potential self-welding between adjacent fuel elements at temperatures

approaching the melting point of the free phase silicon in the coating. Work during this quarter consisted primarily of evaluating improved specimens with respect to these problem areas. These specimens include the admixtured/shelled types FA-16 and FA-23 and the admixture type FA-8. These specimens are described in Table 2-1.

3.1.1 Physical Evaluation of SiC-Si Coated Specimens

The most promising Si-SiC coated specimens as potential candidates for irradiation in Capsule SP-5 were the FA-23 type (1/8 inch unfueled shell) and the FA-16 type (1/16 inch unfueled shell). The shells on these specimens have been found to be well bonded to the fueled cores. Both types are improved over an earlier version in that no evidence of incipient flaws in the graphite have been found, both by destructive visual inspection and nondestructive radiography. Figure 3-1 shows radiographs of a number of views of the specimen selected for irradiation in Capsule SP-5. Six views are shown, each view being taken with the sphere rotated 60° so that complete coverage of the unfueled shell was obtained. No evidence of any cracks can be noted.

Other tests on these specimens included the hot oil test for coating integrity and an alpha assay for surface uranium contamination. Eleven specimens were individually immersed in silicone oil at 375° F. One specimen emitted a single very fine bubble stream and there was no evidence of leakage on the remaining ten specimens. The results of the alpha assay of five specimens are given in Table 3-1. Three positions each equal to 1/7 of the total surface area were checked on each sphere. In Table 3-1, each count rate has been multiplied by 7 and the corresponding fraction of the total uranium in each sphere which is on the outer surface of the coating is listed.

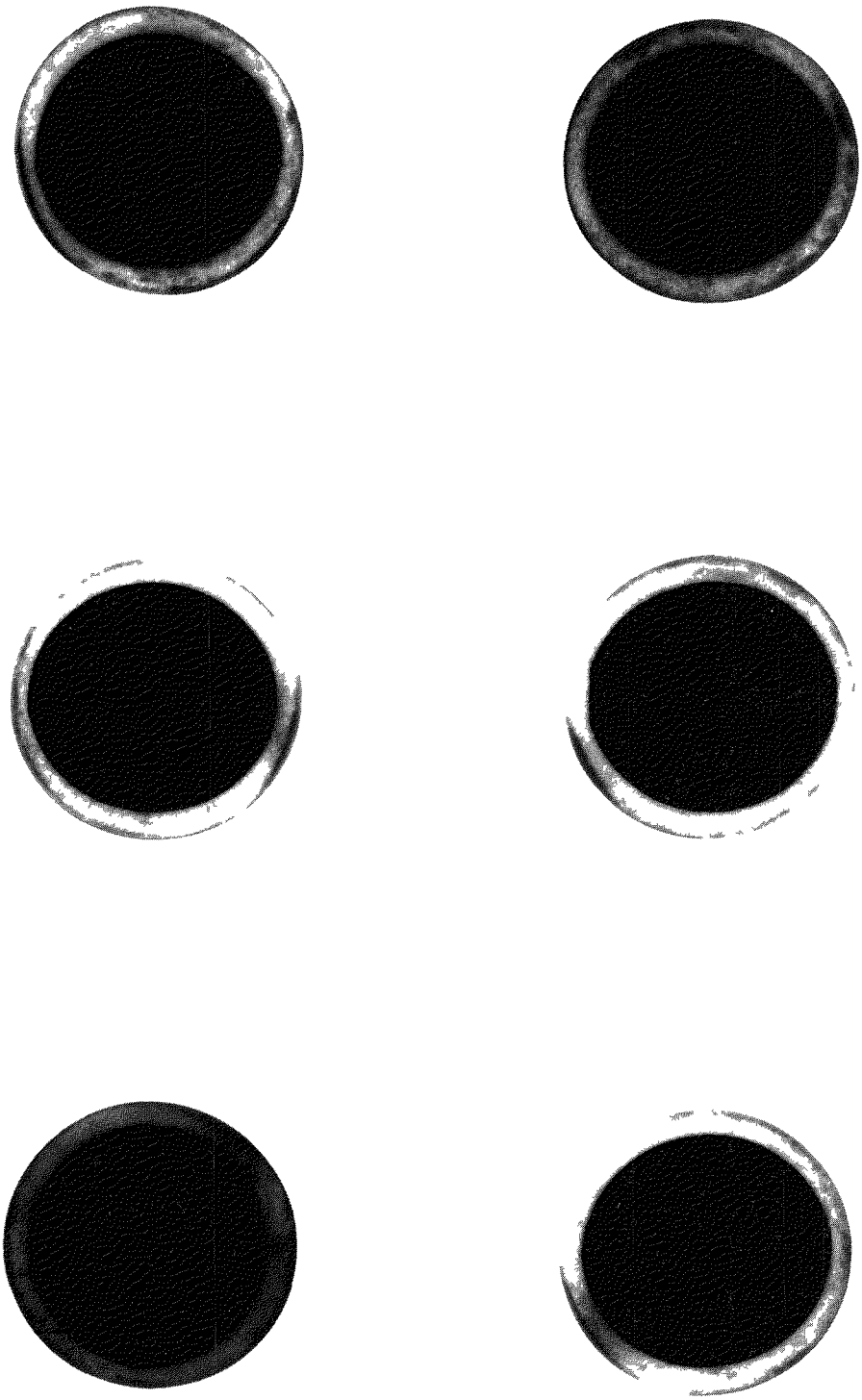

Fig. 3-1. Radiographs of Specimen FA-23 (E8-7)

TABLE 3-1

SURFACE URANIUM CONTAMINATION
OF SiC-Si COATED SPECIMENS

Sphere No.	Position 1	Position 2	Position 3
FA-23 (E8-7)	nil	4.0×10^{-7}	2.3×10^{-7}
FA-23 (E8-12)	2.3×10^{-7}	2.3×10^{-7}	3.1×10^{-7}
FA-23 (E8-1)	1.6×10^{-7}	nil	2.3×10^{-7}
FA-23 (SPE-2)	1.1×10^{-6}	1.9×10^{-6}	3.0×10^{-6}
FA-16 (E16-4)	8.4×10^{-6}	4.4×10^{-6}	7.0×10^{-6}

Slightly higher uranium contamination can be noted in the FA-16 specimen which indicates that there may have been greater uranium migration through the thinner graphite shell of this specimen.

Another self-welding test was run on an unfueled graphite sphere having a similar SiC-Si coating to the FA-16 and FA-23 types. Previous tests had shown no evidence of self-welding at 2000° F but definite evidence was observed at 2500° F. The test sphere was cut in half and the coatings on the two halves placed under a point contact load of 50 lbs. The latest test was run at 2300° F for 50 hrs. This time, there was no evidence of silicon migration or other tendency to self-weld, however, a slight crushing at the point of contact was noted. Since no self-welding was observed, it indicates that a safe upper temperature for this type of SiC-Si containing about 40 v/o free silicon will be about 2300° F.

Another type of SiC-Si coated specimen (FA-8) had been under irradiation in Static Capsule SP-4 to assess the long-term irradiation effects on a coated specimen, particularly the question of whether radiation-induced graphite shrinkage will weaken the specimen. This irradiation started in August, 1959 and was completed this quarter. The design and operating conditions for Capsule SP-4 are described in Section 5.1. The Hot Cell examination of the irradiated specimen was undertaken in this quarter. A summary of the irradiation conditions, weight changes and dimensional changes are given in Table 3-2.

TABLE 3-2

SUMMARY OF IRRADIATION RESULTS
FOR SiC-Si COATED SPECIMEN FA-8 IN CAPSULE SP-4

Heat Generation Rate	2.2KW
Measured Graphite Block Temp.	1400° F
Calculated Surface Temp.	1750° F
Calculated Center Temp.	1850° F
Burnup	7400 KWH
Weight, Pre-Irradiation and Change During irradiation	56.2085 gms, +0.14%
Diameter, Pre-Irradiation and Change During Irradiation	1.5009", +0.43% 1.5683", -0.16% 1.4908", +0.65%

Machined flats could not be used for dimensional measurements on this coated specimen as was done for the uncoated specimens. Instead, grease pencil marks were made at the points of measurement. However, it was noted that repeated measurements at the same diameter showed that dimensional changes were very sensitive to micrometer position. Thus, little significance can be placed on the dimensional changes reported in Table 3-2. The gain in weight of the specimen during irradiation is most likely associated with the crack which was subsequently found in SiC-Si coating. The SiC-Si coating was applied to the graphite sphere at 3600° F in an inert atmosphere which effectively outgasses the graphite matrix before it is coated. Thus, when the coating cracked, it was probable that capsule gas (helium) or atmospheric air (after capsule opening but before weighing) could be readsorbed on the graphite matrix, causing weight gain.

Visual examination of the FA-8 specimen showed it to be crack-free and otherwise sound. However, upon immersing the sphere in 375° F silicons oil, a line of bubble streams clearly showed a single surface crack about 1/4 in. long. Subsequent macroscopic examination confirmed the presence of the crack.

Figure 3-2 is a 4x view of this crack. In view of the importance of trying to determine the cause of this crack, a scheduled impact test on the specimen was omitted. The FA-8 specimen was mounted in plastic so that it could be sectioned and polished to further study the crack. Examination of the polished section actually revealed three cracks through the coating. Two of the cracks were quite large and obviously would have shown in the hot oil test. It was likely that the cutting and polishing operation caused these cracks. The third crack is shown in Figure 3-3. There is not conclusive evidence that this is actually the crack previously observed in the hot oil test since in mounting the sphere in plastic, the orientation of the crack may have been lost. However, it does not have the large, jagged appearance of the other two cracks and is therefore believed to be the crack of interest. As can be noted in Figure 3-3, the crack appears to be along the SiC grain boundaries. The crack was probably caused by a stress in the coating which either resulted from the internal temperature gradient in the specimen or from an initial coating flaw in fabrication which did not leak in the pre-irradiation hot oil test but which propagated under the operating conditions. No evidence of coating separation from the graphite matrix can be noted in Figure 3-3. This is significant because it was thought that radiation induced shrinkage of the graphite matrix might have produced some coating separation. Except for the crack, there is no other visible evidence of a radiation induced change to the Si-SiC material.

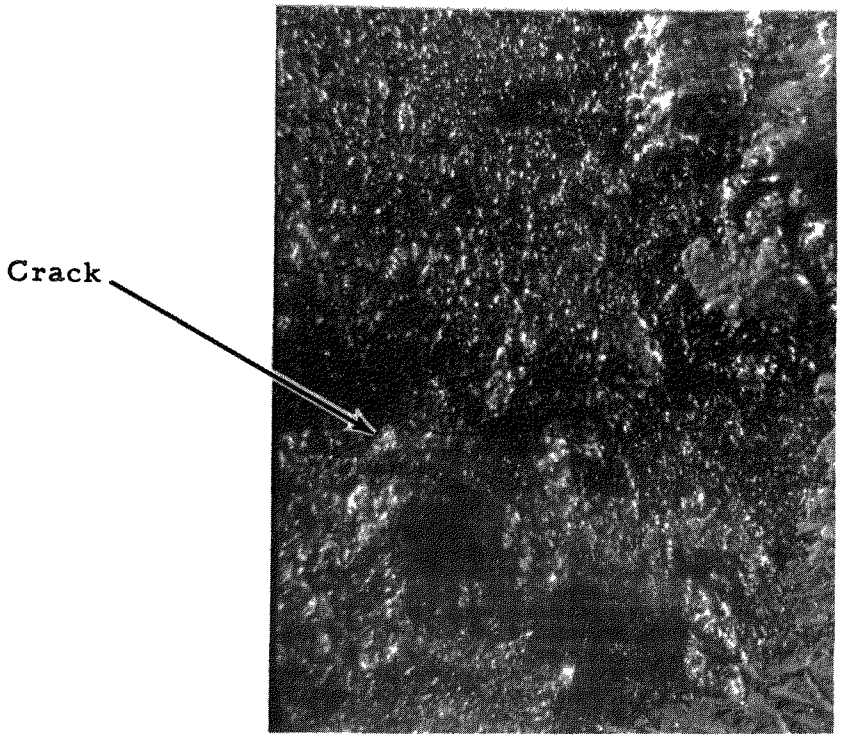

Fig. 3-2. External view (34x) of crack in Si-SiC coating of specimen FA-8 (E6) after irradiation in Capsule SP-4.

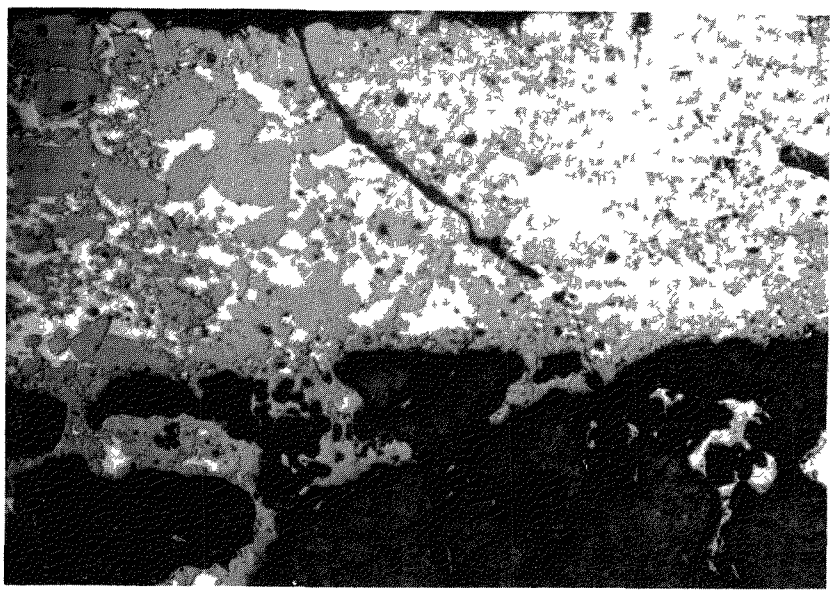

Fig. 3-3. Crack in Si-SiC coating of specimen FA-8 (E6) after irradiation in Capsule SP-4. View at 100x.

3.1.2 Fission Product Retention by Si-SiC Coatings

Coated specimens of the FA-16 and/or the FA-23 types were tested for fission product retention during this quarter by three different tests - neutron activation, furnace capsule, and sweep capsule.

Furnace capsule SPF-2 contained an FA-16 specimen, fueled with normal enrichment uranium. A total of 13 off-gas samples from this experiment were analyzed for long-lived noble fission product gases covering an operating temperature range of 200° F to 1900° F. Initial operation of this capsule was in a thermal flux of 1.7×10^{10}. The fission product retention was so good for this specimen that the capsule was ultimately moved into a flux of 3×10^{12} to achieve maximum sensitivity.

TABLE 3-3

SUMMARY OF FISSION PRODUCT RELEASE DATA
FOR Si-SiC COATED FA-16 SPECIMEN IN CAPSULE SPF-2

Sample No.	Temp, °F	Flux n/cm^2-sec	R/B, (Rate of Release/Rate of Production) Xe 133	Xe 135	Kr 85m	Kr 87	Kr 88
1	200	1.7×10^{10}	← (No detectable release) →				
2	1000	"		"	"	"	
3	1000	3×10^{11}		"	"	"	
4	1000	"		"	"	"	
5	1000	"		"	"	"	
6	1500	3×10^{12}	6.1×10^{-6}	6.1×10^{-7}	5.1×10^{-7}	$< 1.3 \times 10^{-7}$	3.0×10^{-7}
7	1500	"	2.8×10^{-6}	2.0×10^{-7}	8.1×10^{-7}	" "	2.7×10^{-7}
8	1500	"	2.1×10^{-6}	1.6×10^{-7}	3.1×10^{-7}	"	1.7×10^{-7}
9	1500	"	1.7×10^{-6}	1.1×10^{-7}	3.1×10^{-7}	"	1.7×10^{-7}
10	1900	"	2.6×10^{-6}	3.8×10^{-7}	6.7×10^{-7}	"	1.5×10^{-7}
11	1900	"	4.5×10^{-6}	4.2×10^{-7}	4.1×10^{-7}	"	1.2×10^{-7}
12	1900	"	8.2×10^{-6}	2.0×10^{-7}	7.0×10^{-7}	"	3.0×10^{-7}
13	1900	"	4.3×10^{-6}	2.5×10^{-7}	4.7×10^{-7}	"	1.0×10^{-7}

As can be noted in Table 3-3, the release rates for these long-lived fission gases are extremely low. No significant effect of temperature on leakage rate can be noted. An alpha assay of this particular sphere indicated a surface uranium contamination of about 5×10^{-7} of the total uranium in the sphere. This factor together with the lack of temperature dependence indicates that the observed "leakage" rates are most probably due to fissioning of the slight uranium contamination on the surface of the specimen.

In preparation for irradiation in Sweep Capsule SP-5, specimen FA-23 (E8-7) was subjected to a neutron activation test. This specimen was activated in an integrated thermal neutron flux of 3.6×10^{13} nvt at ambient temperature and then heated at 2000° F for 4 hours. During this heating period, the Xe 133 release was below the detection limit of 2.2×10^{-7} of the Xe 133 present inside the specimen. Consequently, this specimen was selected for one of the two sweep compartments in Capsule SP-5. An additional specimen, FA-23 (E8-12), was placed in the static compartment.

The design and operating conditions for Capsule SP-5 are described in Section 5.2. Initial samples of the fission product concentration in the sweep helium stream showed detectable activity. It was necessary to increase the trapping time from the usual 2-hour period to 22 hours. The result of this sample (No. 3) is shown in Table 3-4 along with the pertinent operating conditions of the FA-23 specimen.

TABLE 3-4

SUMMARY OF FISSION PRODUCT RELEASE DATA
FOR Si-SiC COATED FA-23 SPECIMEN IN CAPSULE SP-5

Sample No.	Temp, °F Surface	Temp, °F Center	Power, KW	R/B, (Rate of Release/Rate of Production Kr 85m	Kr 87	Kr 88	Xe 133	Xe 135
1	1300	1440	1.6	←(No detectable release)→				
2	1300	1440	1.6	"	"	"		
3	1300	1440	1.6	2.6×10^{-9}	nil	1.5×10^{-9}	5.7×10^{-9}	1.5×10^{-9}

Extremely good fission product retention was achieved by this Si-SiC coated specimen. The release rate is about two orders of magnitude below that which would be predicted from the surface uranium contamination data in Table 3-1 which was at the lower limit of detection of the alpha assay equipment. Sample No. 3 was taken on April 27 at which time the estimated exposure was 750 KWH per specimen. The first sample taken during the next quarter on May 4 showed a marked increase in fission product release. R/B_4 values for the isotopes listed in Table 3-4 were found to range from 10^{-4} to 10^{-3}. There was no evidence of the increased activity levels on the sweep gas prior to startup of the BRR on May 4. However, as the BRR came up to power, the fission product activity immediately increased. This indicates that whatever the type of coating failure that caused the increase of 5 to 6 orders of magnitude in fission product release, it was associated with increase in internal temperature gradient as the specimen came up to power. The exact nature of the coating failure will not be known until Capsule SP-5 is opened for examination in the Hot Cell.

3.2 Pyrolytic Carbon Coatings

This type of coating contains no metal or metal carbide phase and consists solely of carbon deposited on the fuel element surface by the pyrolysis of a hydrocarbon gas. The type of carbon structure which is formed has an extremely low permeability. The bulk density of the coating can be made to closely approach theoretical carbon density, depending upon the temperature of deposition. The main advantage of this type of coating is that the coating itself will not dictate the temperature limit of the whole fuel element but rather it will be set by the properties of the fissile material and the graphite matrix.

The evaluation of three of types of pyrolytic carbon coatings was continued during this quarter. These types varied primarily in thickness and, to some extent, in deposition temperature. The thickest coating was on the FA-21 (fueled) and FX-3 (unfueled) types which had similar coatings deposited in the range of 3300 to 3400° F. The FA-21 specimens were made by depositing the coating on FA-19 specimens. Specimens of the second type (FA-20) which had been evaluated prior to this quarter had coatings ranging from 2 to 5 mils in thickness which were deposited at about 3000° F. More recent versions of the FA-20 type had thicker coatings ranging up to 12 mils and were deposited at about 3200° F. The FA-20 specimens were made by coating FA-19 specimens. Specimens of the third type are represented by the designation FX-5. This type has a thin 0.5 mil coating deposited at about 3000° F. Test results obtained on these three types of coatings are described below.

3.2.1 Physical Evaluation of Pyrolytic Carbon Coated Specimens

Photomicrographs of the three types of pyrolytic carbon surface coatings are shown in Figs. 3-4, 3-5, and 3-6. The FA-20 coating shown in Fig. 3-4 is 5 mils thick. The typical conical growth patterns of pyrolytically deposited carbon can be clearly seen in this picture which was taken under polarized light. Good bonding of the coating to the graphite body was achieved. However, a crack running parallel to the graphite surface can be noted. This type of cracking has been noted in a number of other samples of pyrolytic carbon coating and is due to stresses during fabrication arising from a difference in thermal expansion coefficient of the pyrolytic carbon coating and the graphite sphere. The FA-21 coating shown in Fig. 3-5 is 50 mils thick and has purposely been prepared to be somewhat thicker than the FA-20 coating. Again, the conical growth patterns and the presence of

Fig. 3-4. Pyrolytic carbon coating on specimen type FA-20. View at 250x.

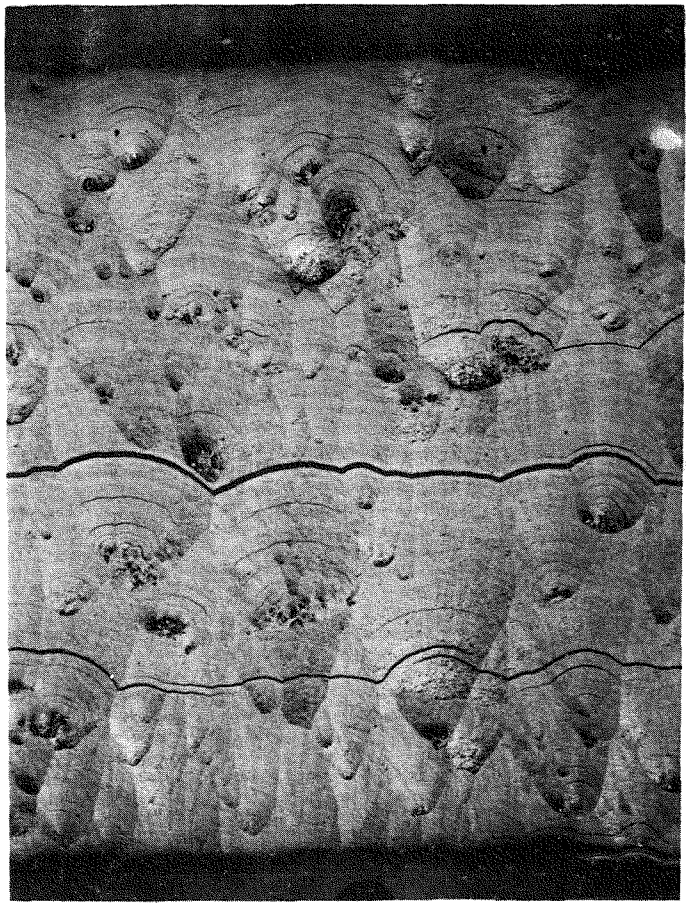

Fig. 3-5. Pyrolytic carbon coating on specimen type FA-21. View at 100x.

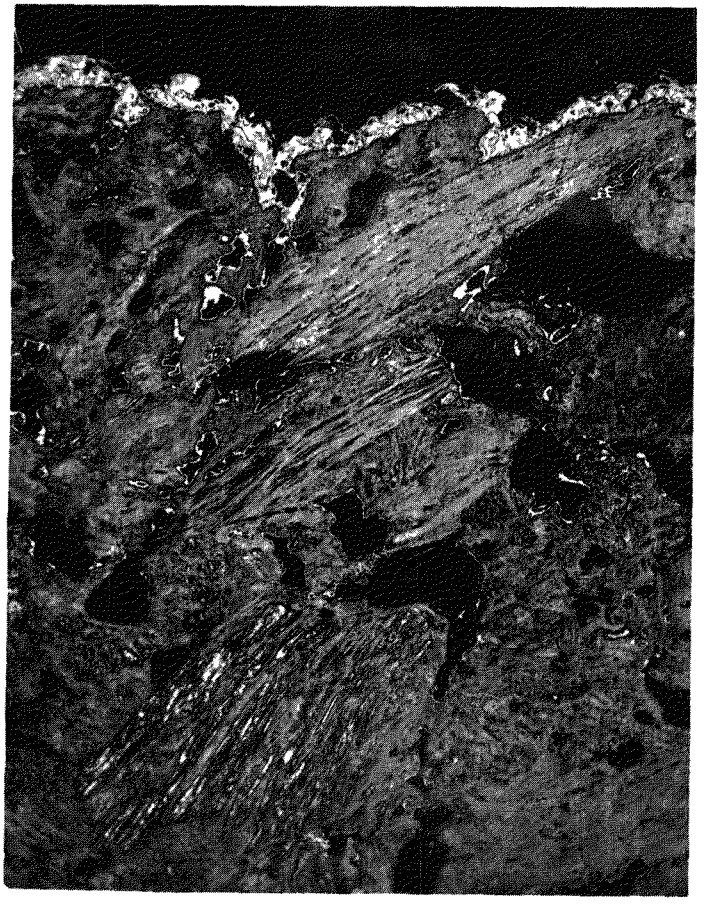

Fig. 3-6. Pyrolytic carbon coating on specimen type FX-5. View at 250x.

cracks parallel to the base plane can be noted. The FX-5 coating in Fig. 3-6 averages only 1/2 mil thick. As noted below, this coating was quite porous but more resistant to impact loads than the FA-20 and FA-21 types.

Most of the pre-irradiation testing of pyrolytic carbon coated specimens during this quarter consisted of hot oil testing for coating porosity and impact testing. Impact test results are summarized in Table 3-5.

TABLE 3-5

IMPACT TESTS ON PYROLYTIC CARBON COATED SPECIMENS

Specimen No.	Coating Thickness, mils	Impact Load, Ft-Lbs. Coating Failure Hot Oil Test	Coating Failure Visual	Graphite Failure
FA-20(433N)	3.4	1.7	1.7	-
FA-20(399N)	4.2	2.2	2.0	-
FX-3(44	50	2.5	2.5	-
FA-21(1N)	50	1.0	1.0	-
FX-5(U2)	0.5	(a)	none	7.0
FA-19(400N)	none	-	-	8.0

(a) Due to coating porosity, additional leaks associated with impact failure could not have been discerned.

The first visual failure on the FA-20(399N) specimen was at 2.0 ft-lbs but the specimen did not leak at this point indicating that an outer portion of the layer had cracked but that the innermost layer remained intact. When the FA-21(N) specimen was impacted at 1.0 ft lbs, a leak was observed by the hot oil test and the impacted area was "spongy" indicating the coating was made up of numerous poorly bonded layers. The thin coating on the FX-5 specimen apparently did not chip off up to the point where the graphite sphere broke.

All specimens of the FA-20 type were found to pass the hot oil leakage test in the as-received condition. In general, most of the thicker coated FA-21 specimens successfully passed the hot oil tests, although one

specimen was found to have a single pinhole type leak. Another FA-21 specimen which had a number of carbon growths about 1/8 inch long protruding from its surface passed the hot oil test. However, when the carbon growths were removed by polishing, pinhole leaks were observed where most of the growths had been. The thin coatings on the FX-5 specimens were all found to be porous by the hot oil leakage test.

Since the pyrolytic carbon is deposited directly on the fueled graphite surface, it was of interest to know whether uranium would migrate through the coating or otherwise contaminate the coating surface. A number of FA-20 specimens were assayed for surface uranium contamination by alpha counting. The results are tabulated in Table 3-6.

TABLE 3-6

SURFACE URANIUM CONTAMINATION
OF PyC COATED SPECIMENS

	Equivalent Fraction of Total U in Sphere		
Sphere No.	Position 1	Position 2	Position 3
FA-20(399N)	2.1×10^{-6}	-	-
FA-20(427N)	1.7×10^{-6}	-	-
FA-20(431N)	5.9×10^{-7}	-	-
FA-20(433N)	7.8×10^{-7}	-	-
FA-20(435N)	1.4×10^{-6}	-	-
FA-20(338E)	7.1×10^{-7}	5.7×10^{-7}	7.1×10^{-7}
FA-20(345E)	5.7×10^{-7}	6.3×10^{-7}	2.3×10^{-6}
FA-20(325E)	4.8×10^{-7}	2.1×10^{-6}	3.2×10^{-7}
FA-20(329E)	1.6×10^{-7}	8.8×10^{-6}	3.2×10^{-6}
FA-20(344E)	1.6×10^{-7}	4.4×10^{-7}	nil

Occasionally, several spots on the sphere have been found to have a somewhat higher uranium contamination but on the whole, it can be seen that there is no serious uranium contamination of this type of coating.

An FA-20 specimen had been subjected to high burnup in Static Capsule SP-4 with the primary objective of determining the effect of irradiation on the pyrolytic carbon material and also to see whether radiation

induced changes to the fueled graphite sphere would weaken the coating in any way. This irradiation started in August, 1959 and was completed this quarter. The design and operating conditions for Capsule SP-4 are described in Section 5.1. The Hot Cell examination of the irradiated specimen was undertaken in this quarter. A summary of the irradiation conditions, weight changes, and dimensional changes are given in Table 3-7.

TABLE 3-7

SUMMARY OF IRRADIATION RESULTS FOR PYROLYTIC CARBON COATED SPECIMEN FA-20(336E) IN CAPSULE SP-4

Heat Generation Rate	2.0 KW
Measured Graphite Block Temp.	1250° F
Calculated Surface Temp.	1550° F
Calculated Center Temp.	1750° F
Burnup	6700 KWH
Weight, Pre-Irradiation and Change During Irradiation	52.2367 , +0.19%
Diameter Pre-Irradiation and Change During Irradiation:	
Position 1	1.4904", -0.17 %
Position 2	1.4948", -0.42%
Position 3	1.4976", -0.31%
Position 4	1.4978", -0.28%
Position 5	1.5028", -0.93%

Visual examination of the specimen upon its removal from the capsule revealed a band of 5 parallel hair line cracks all spaced within a 1/4 inch wide band running completely around the sphere. These cracks can be seen in Figure 3-7. As expected there was profuse leakage from the cracks when the specimen was subjected to the hot oil test. There appeared to be some slight leakage in areas removed from the crack region. However, due to the profuse bubbling from the crack region, the presence of other pinholes could

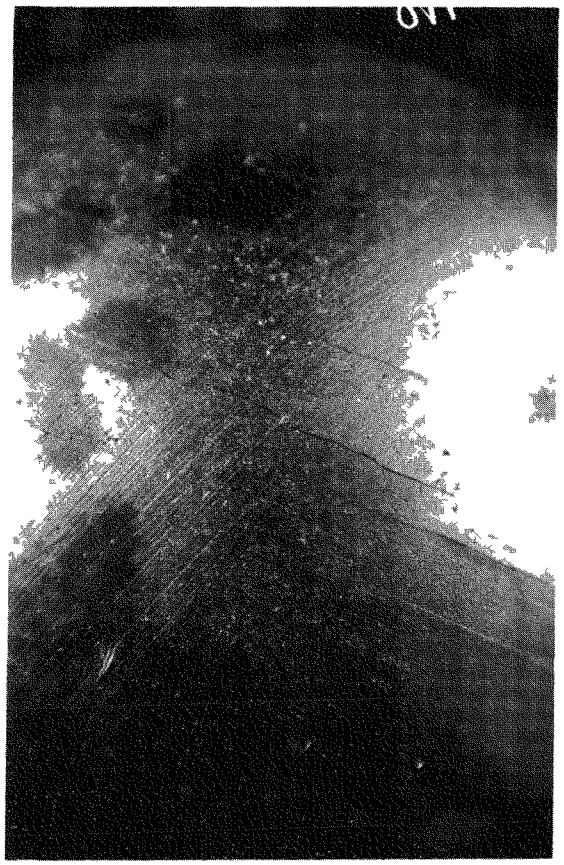

Fig. 3-7. Cracks in surface of pyrolytic carbon coated specimen FA-20 (336E) after irradiation in Capsule SP-4. View at 4x.

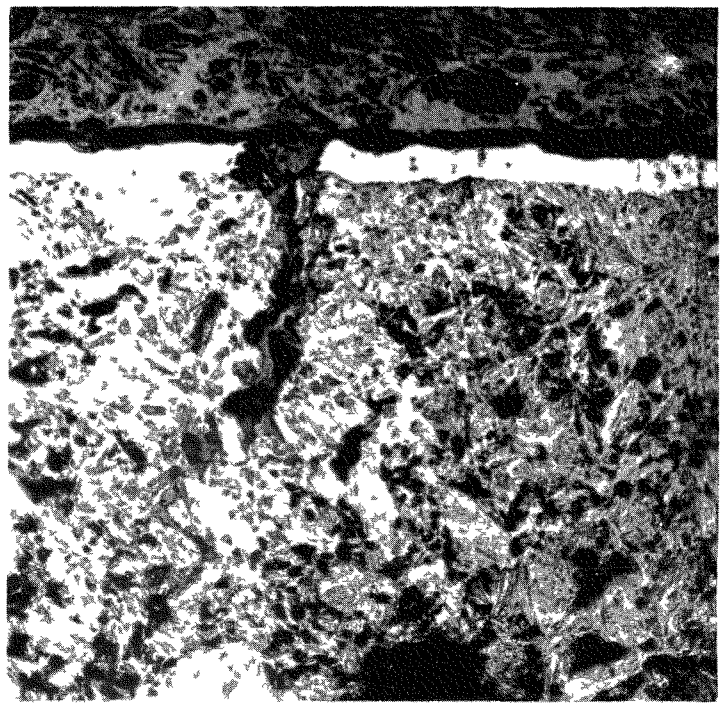

Fig. 3-8. One of the cracks in the surface of pyrolytic carbon coated specimen FA-20 (336E) after irradiation in Capsule SP-4. View at 100x.

not be definitely confirmed. The weight gain listed in Table 3-7 was similar to that observed for the Si-SiC coated specimen also in Capsule SP-4 and is probably associated with the readmission of atmospheric air through the cracks which developed in the coating. In view of the importance of trying to determine the cause of the cracks in the coating, the scheduled impact test on this specimen was omitted. The specimen was mounted in plastic so that it could be sectioned and polished to further study these cracks. Figure 3-8 is section through the coating of the irradiated specimen FA-20 (336E). One of the five cracks in the coating can be seen in this view. The coating appears to have been pulled apart. A surface crack in the graphite beneath the coating can also be seen. Cracks of this type have not previously been noted in the surface of uncoated graphite and it is possible that strains in the coating actually caused this crack in the graphite. Due to the orderly nature of the coating cracks, the most likely cause is a radiation induced differential dimensional change in the graphite which caused a tensile stress in the coating in the region of the cracks. Although there may have been some radiation damage to the coating itself, it is believed that if this were the dominant factor, the crack pattern in the coating would have been more random than the orderly cracks actually observed.

Another FA-20 specimen had been under low level irradiation in Furnace Capsule SPF-1 prior to this quarter. Leakage factors (rate of release/rate of production) for the long lived noble fission product gases (Kr 85m, Kr 87, Kr 88, Xe 133 and Xe 135) at temperatures of 150° F to 1900°F were found to range from 10^{-4} to 5×10^{-2} (4). Experiments at four temperatures were conducted in the following order: 1500°F, 1000° F, 1900° F, and 150° F. The release rate was somewhat higher than anticipated, particularly during the final run at 150° F. Consequently, it was decided to open Capsule SPF-1 in order to examine the specimen. The examination of FA-20 (310N) was conducted during this quarter. Upon removal of the specimen from the capsule, a large number of pits were readily visible in the surface of the specimen as shown in Figure 3-9. The pits are seen to be largely concentrated in the one region of the specimen. They had the appearance of corrosion pits in metal. Many of the pits appeared to be undercut, that is, the underlying graphite had been removed to a greater extent than the pyrolytic carbon surface coating. From these observations, it was concluded that the sweep helium stream for transporting fission products from the specimen to the trapping system must have become contaminated with oxygen or moisture. Although the gas stream was not analyzed for contaminants, some difficulty had been experienced during the shakedown on Capsule SPF-1 with cold trap plugging due to excessive moisture believed to come from the particular helium tank is use at that time. It is probable that the rate of attack did not become excessive until the 1900° F run, causing the significant release rates during the subsequent 150° F run.

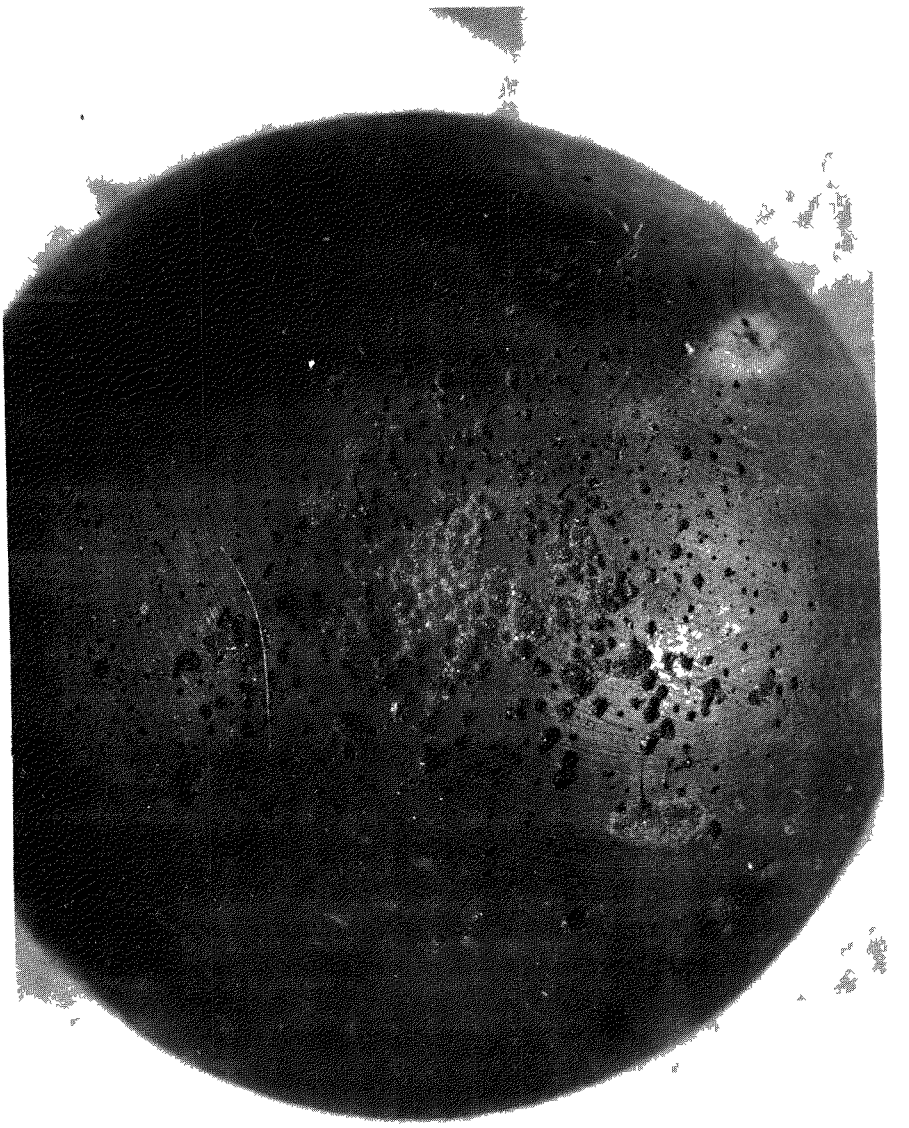

Fig. 3-9. Corrosion pits in surface of pyrolytic carbon coated specimen FA-20 (310N) after exposure in Furnace Capsule SPF-1.

3.2.2 Fission Product Retention by Pyrolytic Carbon Coatings

One of the potential candidates for fission product retention studies under high level irradiation in Sweep Capsule SP-5 was the FA-20 type. Specimen FA-20 (338E) having a 9.5 mil thick pyrolytic carbon coating was subjected to the neutron activation test to determine whether it might be suitable for Capsule SP-5. After activation the specimen was heated at 1900° F for 3 hours during which time the Xe 133 release was less than the detectable amount of 9.3×10^{-7} of the Xe 133 present inside the specimen. The thicker coating and slightly higher deposition temperature are probably responsible for the good fission product retention of this specimen. The FA-20 (310N) specimen having a 2 mil coating deposited at 1700° F had a measurable release under neutron activation about two orders of magnitude greater than the 338E specimen.

In spite of the promising performance of this pyrolytic carbon coated specimen, it was not selected for the sweep compartment of Capsule SP-5 because of the cracking which developed in the SP-4 irradiation and the difficulties in the SPF-1 irradiation with other pyrolytic carbon coated specimens, and the most promising performance of the Si-SiC surface coating and Al_2O_3 particle coatings. However, two FA-20 specimens were included in the static compartment of SP-5. The design and operating conditions for this capsule are described in Section 5.2.

3.3 Conclusions Concerning Surface Coatings

To date, a total of ten PBR fuel element specimens with surface coatings have been or are being subjected to varying levels of high level irradiation in the Capsule program. Of this number, cracks or pinholes have been found in six of the coatings. One specimen (FA-8 in Capsule SP-3) was found to have no pinholes or cracks and the condition of the three other specimens (one FA-23 and two FA-20 in the static compartment of Capsule SP-5) are presently unknown. The exact causes of the failures are not known precisely but evidence indicates that the graphite matrix contributed to most of the failures, either through incipient flaws in the graphite or through dimensional changes of matrix under irradiation.

It is indeed unfortunate that the failure statistics to date are so oppressive because at least one of these materials has been found to be an excellent barrier to fission product diffustion, a property heretofore thought to be solely in the realm of metallic claddings. Release factors of the order of 10^{-9} for the Si-SiC coating under high level irradiation existed for a period of about 1 month. Indeed, this fission product retention by the Si-SiC above 1200° F coating temperature probably would exceed that of many metals if the metals were subjected to similar tests. Previous tests have shown that an Si-SiC coated specimen can meet all the pre-irradiation strength requirements and that the coating is well bonded to the graphite matrix. This coating will have a temperature limitation slightly in excess of 2000° F due to migration of the free phase silicon from the coating. Future work would have to include a detailed understanding of the properties of the underlying graphite body that could cause coating failure and a rather large quantity of specimens would have to be fabricated and tested in order to insure statistical confidence with this type.

The pyrolytic carbon coating has shown some promise as a fission product barrier in several neutron activation. It has the advantage of overcoming the temperature limitation inherent in the Si-SiC coating. However, it appears that while relatively thick coatings are necessary to achieve good fission product retention, interlayer cracking in these thicker coatings seriously weakens the coating. As with the Si-SiC coating, a better understanding of the graphite matrix and the evaluation of a large quantity of specimens would be required before this type of coating could be utilized.

4.0 Coated Fuel Particles

Another method of retaining fission products in a uranium-graphite fuel element is to place a coating on each individual fuel particle of an admixture type element. There are several advantages of coatings on fuel particles. Fission products are retained at their source. The coating material is not subjected to such external loads as impact, compression, or abrasion, nor such internal loads as thermal stress which are normally applied to a PBR fuel element. The fracture of a PBR fuel element will not expose uncoated fuel particles, thus fission product retention will be largely maintained. There should be a minor beneficial effect on manufacturing costs since the graphite fabricator will not have to handle exposed fuel. There may well be an advantage in reprocessing in that the graphite matrix can be removed and disposed of with little regard for the contained uranium and fission products inside the particle coatings.

Several types of fuel particle coatings were investigated prior to this quarter. One type was a sintered Al_2O_3 coating on UO_2 which showed promising fission product retention but seemed to require excess coating thickness to enable reproducible batches to be made (4). Several types of metallic coatings on UO_2 were also investigated. These include Ni, Nb, and Ni-Cr, but it was found that reactions with graphite completely destroyed the coating (3). Work was started during the previous quarter on another type of Al_2O_3. Initial work with this vapor-deposited Al_2O_3 by the Battelle Memorial Institute showed that it overcame the fabrication problems of the sintered Al_2O_3.

During the present quarter, work was continued on vapor-deposited Al_2O_3 on UO_2 at Battlle and a new program on pyrolytically deposited carbon coatings (PyroC) on UC_2 was started, also at Battelle. The interest in PyroC stems from some of the fission product retention results in the PyroC surface coating program (see Section 3.2) together with the facts that a PyroC coating on a fuel particle would not displace the moderator and it would not react with the graphite matrix. A third type of coating which is being considered for future work is BeO. It is believed that BeO can be vapor-deposited on UO_2 to form coatings as dense and impermeable as Al_2O_3. In addition, BeO is reported to react at a higher temperature with carbon than with Al_2O_3 (8). A BeO coating effectively replaces the graphite moderator that it displaces and actually enhances the neutron cycle through the n-2n reaction.

Most of the work on particle coatings has been with Al_2O_3. Fabrication, screening tests and radiation tests of Al_2O_3 coated UO_2 and fuel elements are described in Section 4.1. The PyroC coated UC_2 particle work is described in Section 4.2.

4.1 Vapor-Deposited Alumina Coatings

This type of coating is deposited on the surface of fuel particles from a vapor phase reaction. A bed of UO_2 particles is fluidized by an inert carrier gas containing aluminum chloride vapor. The aluminum chloride is reduced by hydrogen in the presence of water vapor so that a dense impermeable coating of Al_2O_3 is deposited on the UO_2 particles. The large number of particle collisions, during the fluidized coating process, each tending to form a new growth site, is thought to be a major factor in forming the dense coating. No further sintering is required after the fluidization process. In the 1000°C - 1100°C range in which particles have been coated to date, alpha-phase Al_2O_3 is formed. The deposition temperature appears to be the most significant variable in the work to date since lower temperatures tend to produce porous coatings. Other process factors which could be significant but which remain to be explored include gas composition, flow rate, and bed height.

Five batches of Al_2O_3 coated UO_2 have been prepared. The pertinent characteristics of each batch are shown in Table 4-1. The batches which have been used to fuel graphite spheres are also shown.

TABLE 4-1

Al_2O_3 COATED PARTICLES & FUELED GRAPHITE SPHERES MADE TO DATE

Batch No	UO_2 Size, μ	Uranium Enrich.	Coating Thick., μ	Deposit. Temp.	No. of Spheres
1	105/149	Nat.	20	1830°F	3
2	105/149	Nat.	38	1830	2
3	105/149	Nat.	50	2010	0
4	105/149	Enr.	55	1830	3
5	250/420	Dep.	40	2010	0

The 20 micron thick (batch No. 1) and 38 micron thick (batch No. 2) Al_2O_3 coatings on UO_2 are shown in Figures 4-1 and 4-2 respectively. Batch No. 2 was made using a portion of batch No. 1 as the starting material. As can be noted, all UO_2 particles are quite uniformly coated with dense continuous Al_2O_3. The coatings in batch No. 1 were applied in three successive steps. As can be noted in both Figures 4-1 and 4-2, good bonding is achieved between succesive layers. The knob formations in Figure 4-2 are not objectionable. The cause of these knobs is not presently known,however it is interesting to note that similar formations have been observed in molecular carbon deposits (i.e. pyrolytic graphite).

Figure 4-3 and 4-4 are 100x and 500x magnifications from batch No. 4, the material presently being irradiated in Capsule SP-5. This coating was applied in five succesive steps. A darker band is seen at the third layer. This darker region was undoubtedly caused by a shift in one or more of the process conditions while depositing the third layer. Again, all layers appear well bonded to the previous layers. More evidence of dark layers was found in batch No. 3.

4.1.1 Physical Evaluation of Al_2O_3 Coated UO_2

A number of screening tests have been used to characterize each batch prior to further irradiation testing. These include a hot air coating integrity test, an alpha assay for uranium contamination, and thermal cycling. In addition, potential reactions between Al_2O_3 and graphite have been studied. In the hot coating integrity test, the particles are exposed to air at 1200°F so that any faults in the coatings will cause the UO_2 to oxidize to U_3O_8. Thus, weight gain is a measure of the lack of coating integrity. This test can also be used to remove faulty particles from production batches since expansion of UO_2 to U_3O_8 causes the coating to further rupture. A leaching and separation process can then remove the faulty particles from the otherwise good batch.

All batches in the as-fabricated conditions have been subjected to the hot air test and no weight gains have been found indicating that this coating process can produce 100% perfect batches. Actually, some slight losses in weight have been noted which are attributed to devolatilization of adsorbed moisture or gas.

One problem in fabrication of the particles was uranium contamination of the coating from UO_2 dust abraded from the fuel particles in the initial

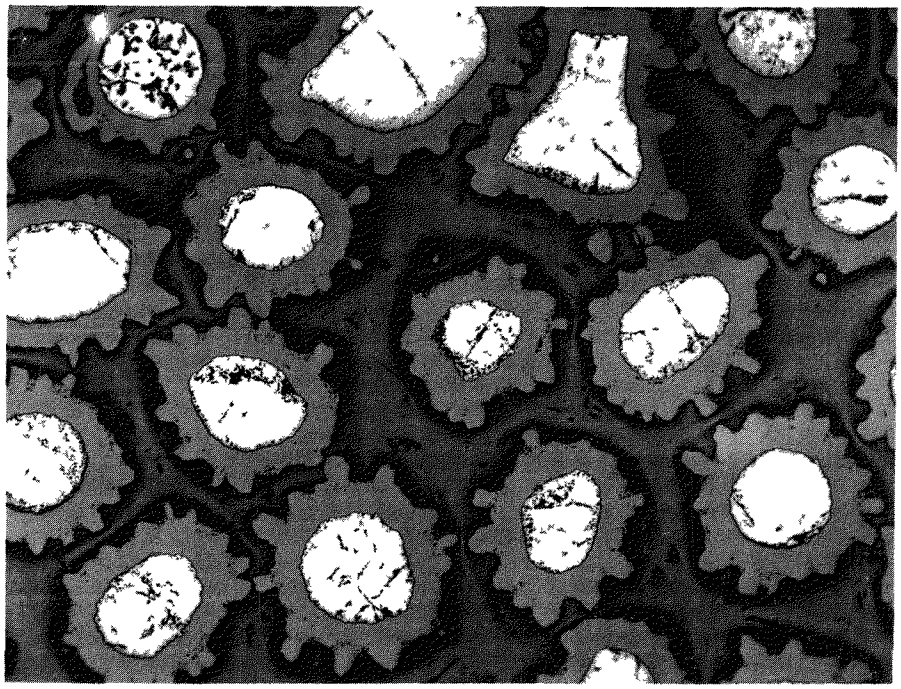

Fig. 4-1. Al_2O_3 coating on UO_2, from batch No. 1. 100x.

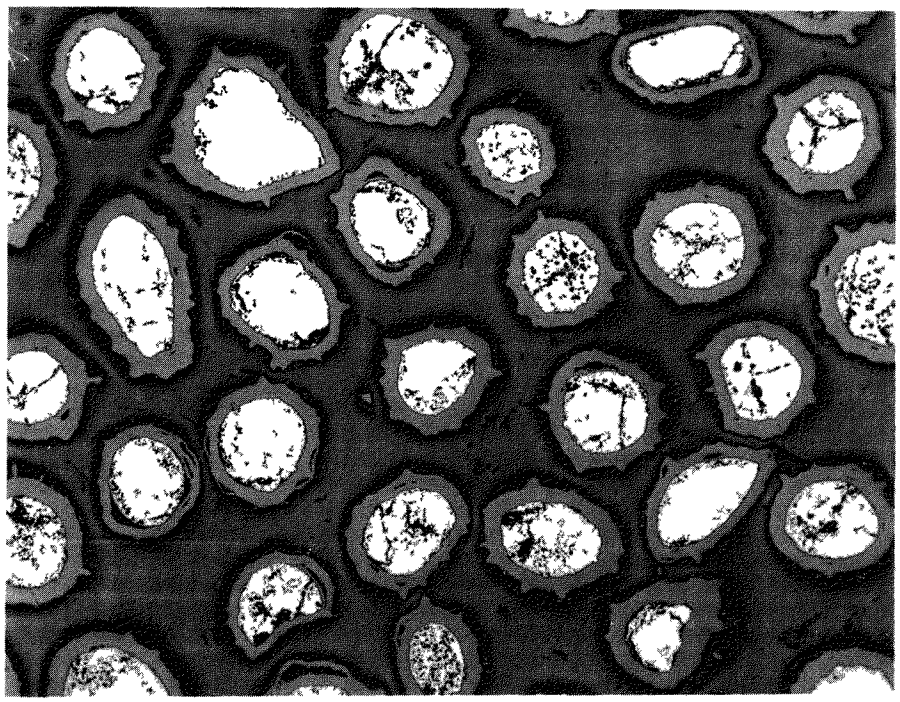

Fig. 4-2. Al_2O_3 coating on UO_2, from batch No. 2. 100x.

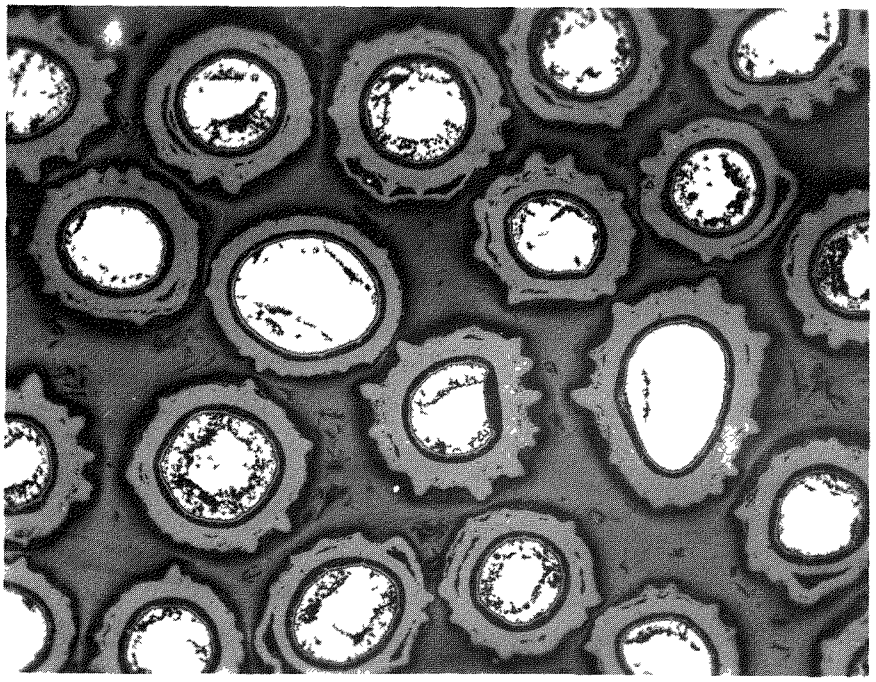

Fig. 4-3. Al_2O_3 coating on UO_2, from batch No. 4 100x.

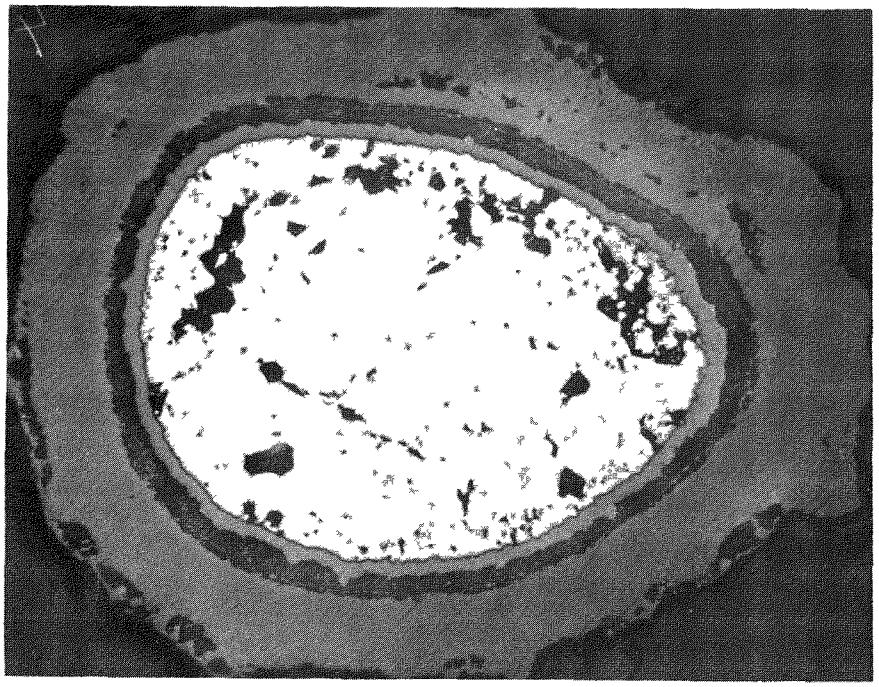

Fig. 4-4. Al_2O_3 coating on UO_2, from batch No. 4. 500x.

stages of coating. This problem was overcome by stopping the process after several microns of Al_2O_3 had been deposited, cleaning the reactor, and restarting. This technique was used on all five batches. Surface contamination of the finished particles was measured by a 2π gas flow alpha counter. Results of the alpha assays are given in Table 4-2.

TABLE 4-2

URANIUM CONTAMINATION ON Al_2O_3 COATED UO_2

Batch No.	Net Alpha Count cpm/gm. particles	Fraction of Total U on Surface
1	7.3 ± 1.3	1.5×10^{-5}
2	1.4 ± 1.0	4.4×10^{-6}
3	0.8 ± 0.8	2.5×10^{-6}
4	20.7 ± 2.5	2.8×10^{-5}

Comparison of batches 1 and 2 shows that a thicker coating on the same material does tend to reduce the surface contamination. The higher count rate in batch 4 is due to the use of enriched uranium in this batch.

Several of the batches were temperature-cycled to see whether the slightly higher expansion coefficient of UO_2 (10×10^{-6}/°C) compared with the Al_2O_3 (8.5×10^{-6}/°C) would cause the particles to rupture when heated above their fabrication temperature. A top test temperature of 2500°F was selected because this appears to be an upper limit on the allowable reaction rate between Al_2O_3 and graphite. The first thermal cycle test was on a portion of batch 2.[3] This test was performed in air. Metallographic examination revealed that some of the coatings had cracked after thermal cycling. An alpha assay of the cycled material showed that fractional surface uranium contamination increased to 2.4×10^{-4} from the value of 4.4×10^{-6} shown in Table 4-2. This thermal cycle test was repeated on another portion of batch 2 and a portion of batch 3 except that this test was done in a reducing atmosphere of N_2 + 10 v/o H_2. Microscopic examination of both batches after testing revealed no cracks in the coating. An alpha assay of the batch 3 material showed an increase over the pre-test value shown in Table 4-2 of only a factor of 2. Thus, thermal cycling to 2500°F of the 105/1249μ UO_2 with a 50μ Al_2O_3 coating in an inert atmosphere does not affect the coating integrity. However, when a portion of batch 5 was thermal cycled to 2500°F in a reducing atmosphere, a subsequent hot air oxidation test caused a 10% weight gain in the sample indicating significant coating failure.

On the assumption that there is no difference in properties of the coating material between the various batches, the failure in batch 5 can be attributed to the lower coating thickness-to-particle diameter ratio of this batch.

One known limitation of the Al_2O_3 coating is its reaction with the graphite matrix. Previous tests with sintered Al_2O_3 coatings (4) in various types of graphite at 2500°F for 1000 hrs. showed that a conventional graphite (graphite flour and coal tar pitch binder) produced essentially no reaction with the Al_2O_3. All types of graphite reacted severely at 3000°F in only 6 hrs. The 2500°F carburization test was repeated with vapor deposited Al_2O_3. It was planned to examine the specimens after 168, 500 and 1000 hr. exposures. The materials tested are listed in Table 4-3.

TABLE 4-3

MATERIALS FOR CARBURIZATION TEST OF VAPOR DEPOSITED Al_2O_3 IN GRAPHITE AT 2500°F.

Sample No.	Al_2O_3 Coating Thickness	Graphite Filter	Pitch Binder	Bake Temp., °F
1	20	AGOT	Barrett	1700
2	20	2301	Coal Tar	2300
3	40	2301	Coal Tar	2300

During this quarter, only the 168 hr. specimens were examined. Some evidence of attack was noted in sample 1. Slight attack was noted in sample 2 and no attack was noted in sample 3. Although final results of this test must be awaited, it appears that the safe operating temperature for Al_2O_3 should be somewhere below 2500°F.

As noted in Table 4-1, a total of eight graphite spheres fueled with Al_2O_3 coated UO_2 were made during this quarter. These spheres have been designated FA-22 (see Table 2-1). The graphite spheres for the FA-22 specimen were made in the same manner as the uncoated UO_2 fueled FA-1 specimen except that the FA-22 specimen was baked at a slightly lower temperature of 2300°F. One question in the fabrication of this type element is whether the mixing and molding process will damage the Al_2O_3 coatings. An alpha assay was made of each of the as-fabricated spheres to investigate this point. The results are listed in Table 4-4. The spheres were counted at three locations, each approximately 1/7 of the total surface area. The results were multiplied by seven to give an equivalent whole surface contamination.

TABLE 4-4

URANIUM CONTAMINATION OF FA-22 SPECIMENS

Specimen No.	Fuel Batch	Equivalent Whole Surface Contamination, mg U		
		Position 1	Position 2	Position 3
FA-22 (436N)	1	.017	.0037	.0019
FA-22(437N)	1	.0037	nil	.0019
FA-22(448N)	2	.011	nil	.022
FA-22(449N)	2	.0037	.0092	.0055
FA-22(39-9N)	1	.022	.0055	.0092
FA-22(470E)	4	.0046	.0076	.060
FA-22(471E)	4	.0065	.0034	.0034
FA-22(472E)	4	.012	.0050	.0046

A contamination of .0095 mg U represents 10^{-6} of the total uranium in the sphere. The location of the uranium contamination, whether it be on the particle surfaces or uniformly dispersed in the graphite matrix, cannot be established from the data in Table 4-4. A better indication of any damage effect is fission product release. A neutron activation test is described in Section 4.1.2 from which it was concluded that there was no significant damage to the particle coatings since the Xe 133 release from the same batch of particles after admixture into graphite spheres showed only a slight increase.

Another question in ball fabrication is the molding flash resulting from the forming operation. This flash is normally removed by a simple machining operation to produce a perfect sphere for capsule irradiation. However, coated particles in the region of the flash could be damaged in this process. The flash was machined off several of the specimens and a subsequent alpha assay showed a two order of magnitude increase in uranium contamination in this region. Thus, the molding flash was not removed from all specimens subjected to fission product retention tests. Further work will be done on die design to minimize molding flash and remove all sharp corners, even though perfect spheres are not required for use in a Pebble Bed Reactor.

The surface of an FA-22 specimen is shown in Figure 4-5. The appearance of numerous particles at the surface can be noted. A final design of this type of element will require some method of insuring that no particles would be lost from the surface of element during operation. Several methods which will be investigated include an unfueled graphite

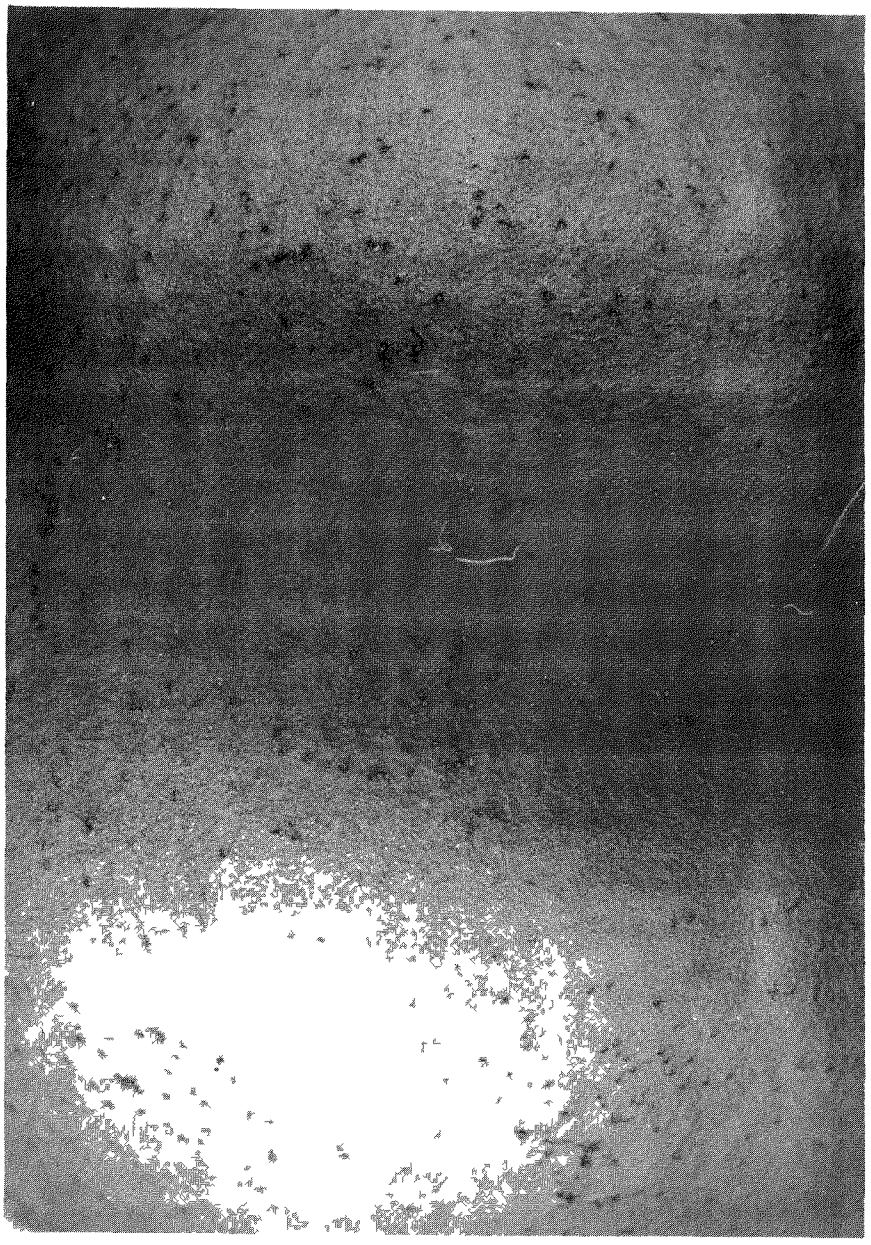

Fig. 4-5. External view of an FA-22 specimen showing Al_2O_3 coated UO_2 particles at the surface.

shell, a thin porous low temperature PyroC coating, and a pre-coating of carbonaceous material on each Al_2O_3 coated particle prior to mixing in the graphite.

The only other physical characterization test performed on the FA-22 specimen was a compression test. Compressive failures of 4465 and 4435 lbs. were found. These values are well above the required 500 lbs. compressive load and are even higher than the average 2500 lb. compressive load found for FA-1 specimens. This indicates that the presence of the particle coatings has not affected the strength of the element. Actually, the increased strength reflects the slightly lower degree of graphitization of the FA-22 specimen.

4.1.2 Fission Product Retention by Al_2O_3 Coatings

The first screening test for fission product retention was a neutron activation test on portions of batches 1 and 2. The results of this test are given in Table 4-5.

TABLE 4-5

NEUTRON ACTIVATION TEST ON Al_2O_3 COATED UO_2

Batch No.	Coating Thickness, μ	Test Temp., °F	Time min.	Fractional Release of Xe133
1	20	1850	100	$<1.7 \times 10^{-4}$
		2250	75	1.7×10^{-4}
		2400	135	1.6×10^{-4}
2	40	1500	144	1.3×10^{-6}
		1500	60	$<3.7 \times 10^{-5}$
		2000	50	$<3.7 \times 10^{-5}$

The Xe133 releases equivalent to the surface uranium contaminations shown in Table 4-2 are 1.5×10^{-5} for the batch 1 material and 4×10^{-6} for the batch 2 material. The total Xe133 release from batch 1 is an order of magnitude greater than predicted from uranium contamination while the release during the first 1500°F run on batch 2 was about equivalent.

Next, graphite spheres fueled with material from batch 1 and batch 2 (Type FA-22 elements) were subjected to the neutron activation test. Results of this test are shown in Table 4-6.

TABLE 4-6

NEUTRON ACTIVATION TEST ON GRAPHITE SPHERES FUELED WITH Al_2O_3 COATED UO_2

Specimen No.	Fuel Batch	Al_2O_3 Coating Thickness, μ	Test Temp, °F	Time, Min.	Fractional Release of Xe133
FA-22(437N)	1	20	1650	80	$<8.1 \times 10^{-6}$
			1800	50	1.6×10^{-5}
			2200	60	4.9×10^{-5}
			2350	30	2.6×10^{-5}
FA-22(449N)	2	40	1500	270	7.5×10^{-6}
			1900	60	$<9.4 \times 10^{-6}$
			1900(a)	60	$<9.4 \times 10^{-6}$
			1900(a)	135	$<9.4 \times 10^{-6}$

(a) Prior to these runs, the specimen was cooled to 600°F in 7 min. and reheated to 1900°F in 10 min.

Rather good agreement can be noted between the sphere data in Table 4-6 and the coated particle data in Table 4-5 indicating that the admixture process for fabricating the spheres caused no significant damage to the particle coatings. Lower fission product release was found from the sphere fueled with UO_2 coated with the 40 micron thick Al_2O_3 coating. Also, the thermal cycling between 1900°F and 600°F had no apparent effect on fission product retention.

The FA-22(449N) specimen was selected for further fission product release testing in Furnace Capsule SPF-3. In this test, fission product release rate can be measured while the specimen is under a low level irradiation. Specimen temperature is controlled by an electrical heater. Data from SPF-3 is given in Table 4-7.

Comparison of the 1000°F and 1500°F runs shows some dependence of fission product leakage rate on temperature. These levels of release were sufficiently low to warrant further irradiation testing of the FA-22 specimen in a higher flux in Sweep Capsule SP-5.

TABLE 4-7

FISSION PRODUCT RELEASE FROM Al_2O_3 COATED UO_2 FUELED SPECIMEN FA-22(449N) IN FURNACE CAPSULE SPF-3

Sample No.	Flux, nv.	Temp. °F	R/B, Rate of Release/Rate of Production Kr 85 m	Kr 87	Kr 88	Xe 133	Xe 135
1	2×10^{12}	150	← (No detectable release) →				
2	"	1000	5.6×10^{-7}	4.2×10^{-7}	2.6×10^{-7}	1.2×10^{-6}	1.7×10^{-7}
3	"	1500	2.0×10^{-6}	1.0×10^{-6}	3.2×10^{-7}	5.8×10^{-6}	1.7×10^{-6}

The specimen selected for the high level irradiation was FA-22(471E) which was fueled with particles from batch 4. This specimen was first subjected to a neutron activation test. At 1950°F, only 7.7×10^{-6} of the Xe 133 in the sphere was released in 4 hours and consequently this specimen was encapsulated in one of the sweep compartments of Capsule SP-5. The design and operating conditions for Capsule SP-5 are described in Section 5.2.

Three gas samples were taken from the FA-22(471E) specimen during this quarter. The results are given in Table 4-8.

TABLE 4-8

FISSION PRODUCT RELEASE FROM Al_2O_3 COATED UO_2 FUELED SPECIMEN FA-22(471E) IN CAPSULE SP-5.

Sample No.	Surface Temp, °F	Specimen Power, KW	R/B, (Rate of Release/Rate of Production) Kr 85m	Kr 87	Kr 88	Xe 133	Xe 135
1	1200	1.3	2.2×10^{-8}	$<5.0\times10^{-9}$	2.2×10^{-9}	1.8×10^{-7}	1.9×10^{-8}
2	1200	1.3	8.0×10^{-8}	1.8×10^{-8}	2.7×10^{-8}	1.0×10^{-7}	4.0×10^{-8}
3	1360	1.5	6.4×10^{-7}	1.8×10^{-7}	2.9×10^{-7}	1.9×10^{-6}	4.9×10^{-7}

These first results for the FA-22 specimen under high level irradiation are most encouraging. Again, some evidence of the dependence of fission product leakage rate on temperature is seen when comparing sample #3 with sample #2. It is planned to continue operation throughout the next quarter. During this time, the special underwater trap for detecting non-volatile fission leakage will be operated.

4.2 Pyrolytic Carbon Coatings on Fuel Particles

An exploratory program on PyroC coatings on individual fuel particles was started during this quarter at Battelle. The process is similar to that used on PyroC surface coatings (Section 3.2). A bed of UC_2 particles is fluidized by a helium stream containing a hydrocarbon gas such as methane or acetylene. By externally heating the fluid bed, the hydrocarbon gas decomposes and carbon is deposited on the surface of the particles.

Two batches were produced during this quarter. UC_2 particles for these batches were obtained by crushing and sieving a UC_2 pellet which produced irregularly shaped particles in the 177/250μ size range. A description of these two batches is given in Table 4-9.

TABLE 4-9

DESCRIPTION OF PYROLYTIC CARBON COATED UC_2 PARTICLES

	Batch #1			Batch #2
UC_2 Size, μ	177/250			177/250
Total coating thickness, μ	40			17
Weight % UC_2	77.8			92.8
Coating Layer	1	2	3	1
Layer Thickness, μ	7	21	12	17
Gas	CH_4	C_2H_2	C_2H_2	C_2H_2
Deposition Temp., °C	1125	1020	1090	1015

Photomicrographs of particles from batches 1 and 2 are shown in Figures 4-6 and 4-7. As seen in both figures, all particles have been rather uniformly coated with a continuous carbon phase in spite of the irregular shapes of the UC_2. One particle from batch 1 in Figure 4-6 has a crack at one end through the inner two coating layers but the outer layer is continuous over the crack. The interface between the coating layers 2 and 3 can readily be detected implying that successive layers of PyroC are not as well bonded as in the case of Al_2O_3.

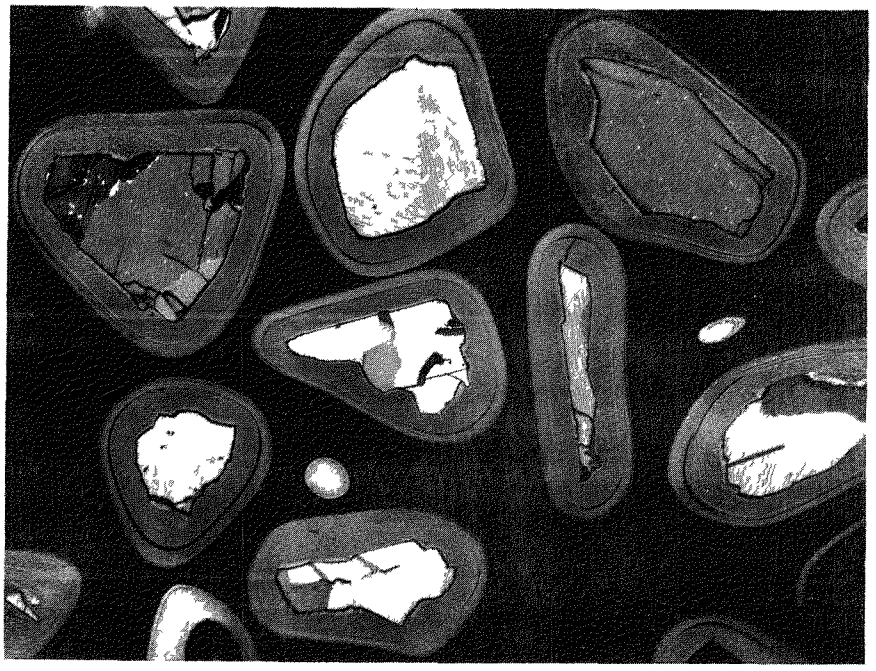

Fig. 4-6. Pyrolytically deposited carbon coating (40 micron) on UC_2 particles. 100x.

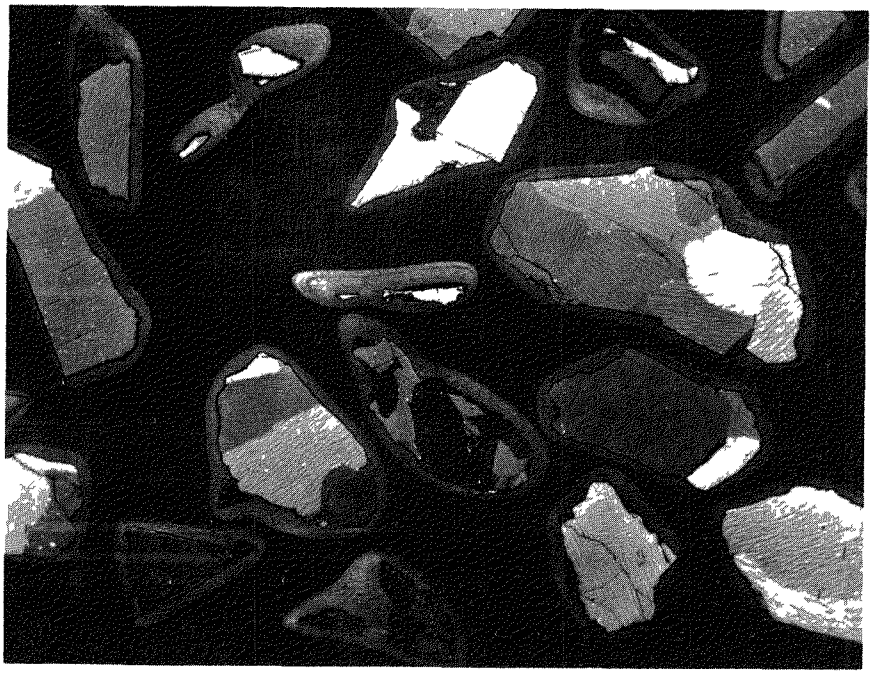

Fig. 4-7. Pyrolytically deposited carbon coating (17 micron) on UC_2 particles. 100x.

4.2.1 Physical Evaluation of PyroC Coated UC_2

The coating integrity of PyroC coated UC_2 particles is tested by immersing the coated particles in hot nitric acid so that uranium can be leached from the particles wherever a coating fault exists. When portions of both batches were tested, no uranium was detected in the leach solution. The limit of detection in this test was 10^{-5} of the uranium in the particles.

The coated particles were next subjected to a thermal cycle test. This test was run at 2000°C because of interest in using the PyroC particle coating to prevent reaction with uranium in an Si-SiC surface coated element. Alpha assays of the test samples were taken both before and after thermal cycling. Results are given in Table 4-10.

TABLE 4-10

ALPHA ASSAY OF PYROLYTIC CARBON COATED UC_2

Batch No.	Net Count Rate Cpm/gm of particles	Surface U / Total U
1 (before cycling)	0.7 ± 1.1	1.3×10^{-6}
1 (after cycling)	2610 ± 31	5.0×10^{-3}
2 (before cycling)	244 ± 7	3.9×10^{-4}
2 (after cycling)	3680 ± 30	5.8×10^{-3}

The assay of the as-fabricated batch 1 showed an extremely low uranium contamination. The rather high reading before cycling for batch 2 probably is due to the 17 micron coating on this batch which is about the alpha coil range in carbon. The increase in alpha count in both batches after thermal cycling was definite evidence of coating failure. Figure 4-8 is a photomicrigraph of batch 2 after cycling where the cracks in the PyroC coating can be seen These cracks are caused by the higher expansion coefficient of the UC_2 compared with the coating. It is expected that this difficulty can be overcome by selecting a coating deposition temperature at the maximum desired operating temperature, by using thicker coatings, or perhaps by exploration of coating properties at higher temperatures.

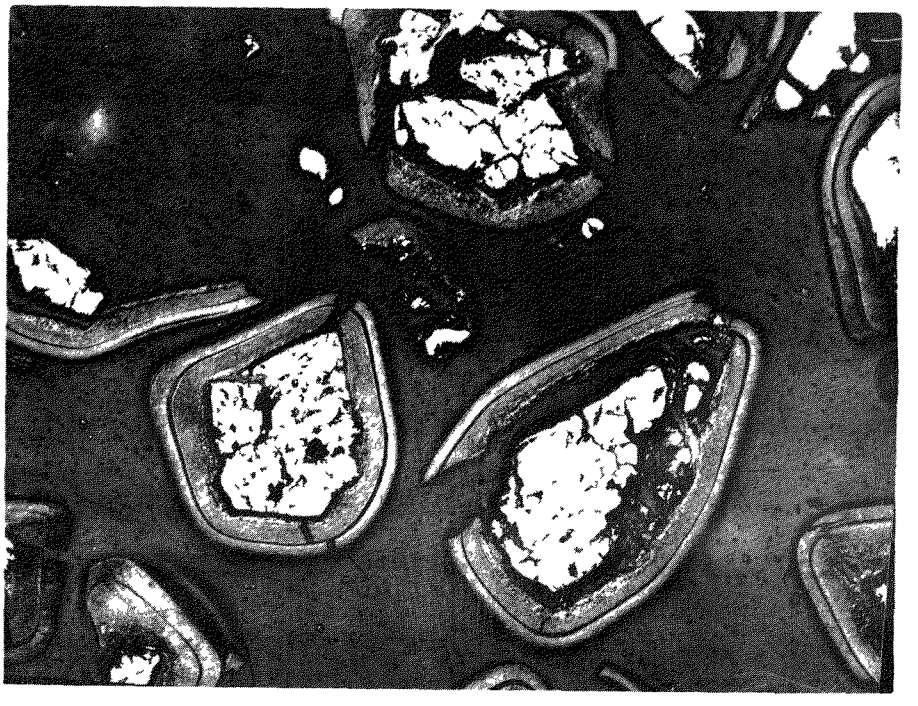

(a) View at 100x.

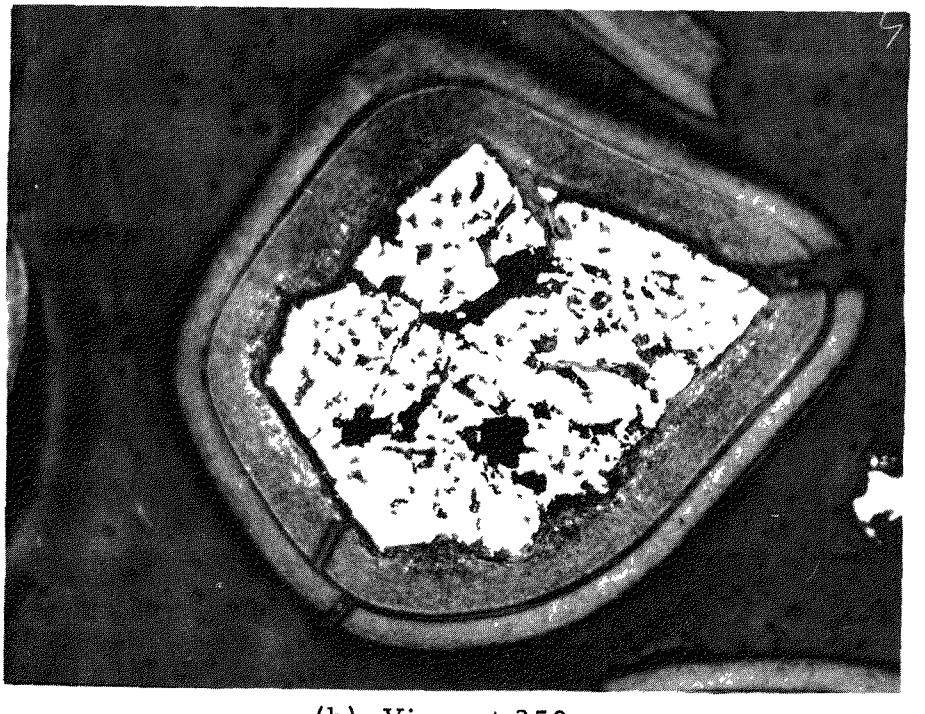

(b) View at 250x.

Fig. 4-8. Pyrolytically deposited carbon coating (40 micron) on UC_2 after thermal cycling to 2000°C.

Some difficulty was encountered with soot formation during the particle coating process at 1000°C - 1100°C. The use of CO_2 to react with excess carbon was tried but found to have no significant effect in decreasing the problem. It is planned to explore higher temperature deposition, the use of spherical UC_2 particles, the incorporation of PyroC coated particles into graphite spheres, and fission product retention characteristics during the next quarter.

4.3 Conclusions Concerning Coated Fuel Particles

The particle coating materials described in this section are unconventional ceramics. Their common characteristic is that, rather than being formed from a sintered compact of granules, they are built up molecule by molecule. This factor is believed responsible for the dense impermeable nature of these coatings. Their obvious advantage over otherwise impermeable metals is that the molecularly deposited ceramics will not be restricted to low temperature applications. They hold promise of achieving the fission product retention of metal claddings used in low temperature reactors while at the same time permitting reactor coolant temperatures that are compatible with modern steam power cycles.

The remarkable factor about the Al_2O_3 coating is that no poor coatings have been produced in any of the batches made to date. A PBR fuel element specimen fueled with this material has exhibited fission product leakage factors of 10^{-9} to 10^{-6} under high level irradiation. Although only a single 1-1/2 inch diameter specimen is being tested, the test takes on added statistical significance because the sphere contains about 500,000 individual "fuel elements" (i.e. coated particles). Although a range of deposition temperatures of only 1000°C to 1100°C has been explored to date, the material produced appears wholly adequate. The mixing and molding steps in the incorporation of coated particles into a graphite matrix do not appear to damage the coatings. Some sort of outer coating will have to be added to the fuel element to prevent loss of particles from the surface. The safe operating temperature of Al_2O_3 will be somewhat below 2500°F which could be adequate for a uniform dispersion of fuel in graphite. It is expected that other coating materials, such as BeO or pyrolytic carbon, having higher temperature limits, will have the impermeability of Al_2O_3. From metallographic examination, the first batch of pyrolytic carbon coatings has the appearance of being dense and impermeable.

The remaining phases of the PBR Fuel Element Development program will emphasize coated fuel particles since fuel particle coatings have shown such good promise and since the surface coatings described in Section 3.0 continue to show a variety of failures which result in fission product release rates which are too high for presently known methods of fission product removal in a primary loop and maintenance techniques.

5.0 Capsule Design and Performance

One incidental advantage of the PBR fuel element concept is the ease of testing full scale fuel elements under conditions closely approaching those of a large power reactor. By replacing the thorium in the reference fuel element with additional enriched uranium, a relatively low powered research reactor such as the 2 MW Battelle Research Reactor can produce power densities in test specimens up to 75% of the desired maximum power denisty. In addition, fission product leakage can be monitored by adding helium inlet and outlet lines to the capsule. Two capsules were under irradiation in the BRR during this quarter: Capsule SP-4 which was a static capsule, and capsule SP-5, which contained two sweep compartments in addition to a static compartment.

5.1 Static Capsule SP-4

The primary purpose of this irradiation was to investigate the stability of UO_2 fueled graphite under high temperature irradiation. Four 1-1/2 in diameter uncoated graphite spheres fueled with different types of UO_2 were included. These specimens and the experimental results on them are described in Section 2.3. Two additional coated specimens were included. These were coated with Si-SiC and pyrolytic carbon and are described in Sections 3.1.1 and 3.2.1 respectively.

The design features of Capsule SP-4 are shown in Fig. 5-1. Since this experiment was concerned solely with the effects of irradiation on physical properties of the specimens, no helium lines were included for detecting fission product leakage. The capsule was designed without auxiliary electrical heaters, depending solely on nuclear heat generation and thermal resistances in the capsule to achieve the desired specimen temperature. Each specimen is mounted in a split graphite cylinder. A 30 mil annulus is provided around each specimen. This annulus is filled with a free flowing graphite powder which minimizes the thermal resistance of the gap while permitting the specimen to expand or contract without restraint. An inconel inner capsule is fitted over the six graphite cylinders. Fins are provided on the outside of the inner capsule. The number of fins and fin thickness were selected to achieve a specimen surface temperature of 1900° F which would result in specimen central temperatures of 2000 to 2100° F. A stainless steel outer capsule is fitted

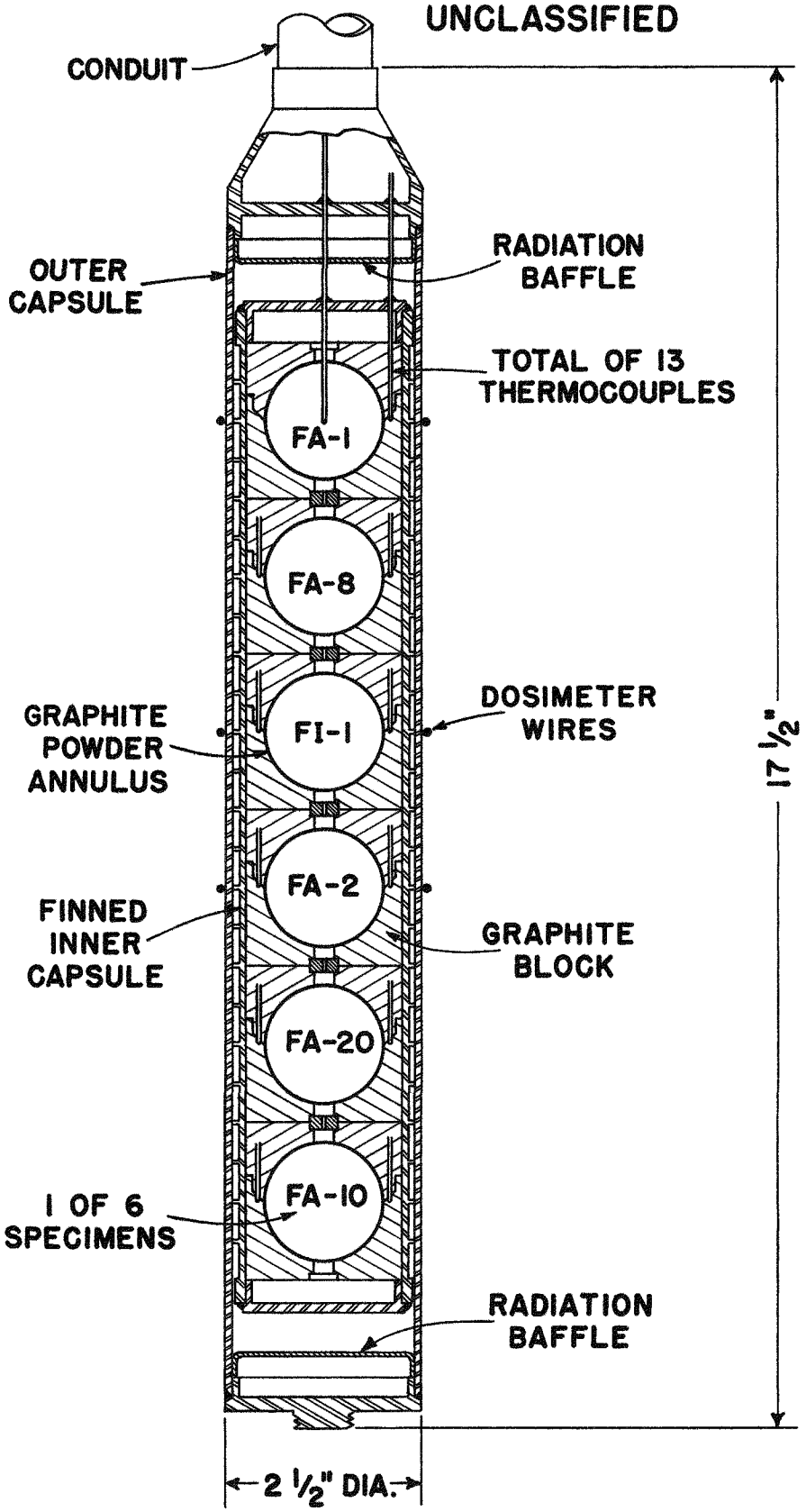

FIG. 5-1 STATIC CAPSULE, SP-4

over the fins. Heat is rejected from this outer capsule wall directly to the BRR pool water. A total of 13 thermocouples were installed in the capsule. Two thermocouples are located in the graphite cylinder just outside the equator of each specimen. In addition, a hole was drilled to the center of the uppermost specimen (Type FA-1) and a thermocouple installed therein. The specimen power level actually obtained can be calculated from the measured temperatures in the graphite cylinder, the pool water temperature, and the effective thermal conductivity of the capsule parts. Using this power level, the specimen temperatures can then be calculated, again starting from the measured graphite cylinder temperature.

Capsule SP-4 was inserted into the BRR on August 25, 1959. Typical operating conditions are summarized in Table 5-1.

TABLE 5-1

OPERATING CONDITIONS FOR CAPSULE SP-4

Specimen	Measured Graphite Block Temp. °F	Ht. Gen. Rate, KW	Calculated Surface Temp.	Central Temp., °F
FA-1 (E82)	1300	1.9	1600	1750 (A)
FA-8 (E 6)	1400	2.2	1750	1850
FI-1 (E 8)	1400	2.3	1750	1850
FA-2 (E 8)	1400	2.2	1750	1900
FA-20 (336E)	1250	2.0	1550	1750
FA-10 (E5)	1300	1.7	1600	1700

(A) Measured temperature. One thermocouple is imbedded in the center of this specimen only. All other central temperatures are calculated.

As can be noted, the target temperature of 1900° F surface temperature was not achieved. Several factors were investigated in an attempt to explain or improve the situation. Since no auxiliary electrical heaters were included, the target temperature was to have been achieved by proper selection of the thickness and material of the various thermal barriers with respect to the anticipated flux levels. One factor was uncovered when laboratory measurements of the thermal conductivity of the Inconel-X used for the inner capsule showed that the literature value used in design was

20% low. An attempt was made to increase the neutron flux by rearranging fuel elements in the BRR core. However, there was no significant increase. Several plans were studied to apply an external thermal barrier to the capsule to increase the temperature. However, the close tolerance required at the capsule-barrier interface appeared impractical to achieve with remote handling devices under 23 ft. of pool water.

The irradiation of Capsule SP-4 was terminated on March 7, 1960. The accumulated full power operating time was 139.5 days. During the course of the irradiation, 6 thermocouples failed, 2 each for the FA-10 and FA-20 specimens, and 1 each for the FA-2 and FI-1 specimens. However, there was sufficient operating time with all thermocouples working so that temperatures where thermocouples had failed could be estimated with confidence based on the thermocouple readings at other locations.

The estimated irradiation exposures for the specimens given in Sections 2.3, 3.1.1, and 3.1.2 were based on the calculated power levels listed in Table 5-1 and the equivalent full power operating time of 139.5 days. Analysis of the cobalt-nickel dosimeter wires for several of the specimens gave somewhat lower values. A comparison of these values is given in Table 5-2.

TABLE 5-2

COMPARISON OF ESTIMATED EXPOSURES TO SPECIMENS IN CAPSULE SP-4 BY TWO METHODS

Specimen	Estimated Exposure, KWH/Sphere	
	From Thermal Data	From Dosimetry
FA-1	6400	3700
FI-1	7700	4400
FA-2	7400	4400

Based on previous experience, burnups calculated from thermal data are usually within ±30% of the dosimetry data. As noted in Figure 5-1, the dosimeter wires are located on the outside wall of Capsule SP-4. The unperturbed thermal neutron flux in the experimental hole was about 3.5×10^{13} and a perturbed flux at the capsule wall should have been about 2×10^{13}. The flux level corresponding to the dosimetry data was only 1×10^{13}. Thus, it is felt that the dosimetry data is probably low but the source of the discrepancy is unexplained.

5.2 Sweep Capsule SP-5

The primary purpose of this irradiation was to investigate the fission product retention characteristics of promising fuel element specimens under high level irradiation. The two most promising specimens selected for Capsule SP-5 were the Si-SiC coated specimen (FA-23) and a specimen fueled with vapor deposited Al_2O_3 coated UO_2 (FA-22).

The design features of Capsule SP-5 are shown in Fig. 5-2. The general method of mounting each specimen in a graphite cylinder and using a doubly contained capsule with fins on the inner capsule is the same as for Capsule SP-4 described in the previous section. However, the outer capsule of SP-5 is divided into two independent compartments. The upper compartment, called the sweep compartment, contains two separate inner capsules. Separate helium inlet and outlet lines are brought to each inner capsule. Gas flow, which is upwards through the graphite powder annulus surrounding each specimen, scavenges any fission products which leak from the specimens and carries them to trapping apparatus outside the capsule. An FA-22 and an FA-23 specimen are located in the two inner capsules of the sweep compartment.

A separate static compartment is located below the sweep compartment. No helium lines are connected to the static compartment. An additional FA-22 specimen, an additional FA-23 specimen, and two FA-20 specimens are included in the static compartment. A simple threaded connection joins the sweep compartment and the static compartment so that if it becomes desirable to examine the sweep compartment specimens (i.e. if large increases in fission product release rates indicate failure of both specimens), the upper compartment can be disengaged and the lower compartment left in the reactor for further irradiation. No thermocouples are included in the static compartment because of this disconnect feature. Temperatures and power levels for these specimens are estimated from temperature data in the sweep compartment and the axial flux profile in the experimental hole.

Irradiation of Capsule SP-5 was started on April 6, 1960 and continued into the next quarter. Two cycles of operation were completed during this quarter. The operating conditions during these two cycles are listed in Table 5-3.

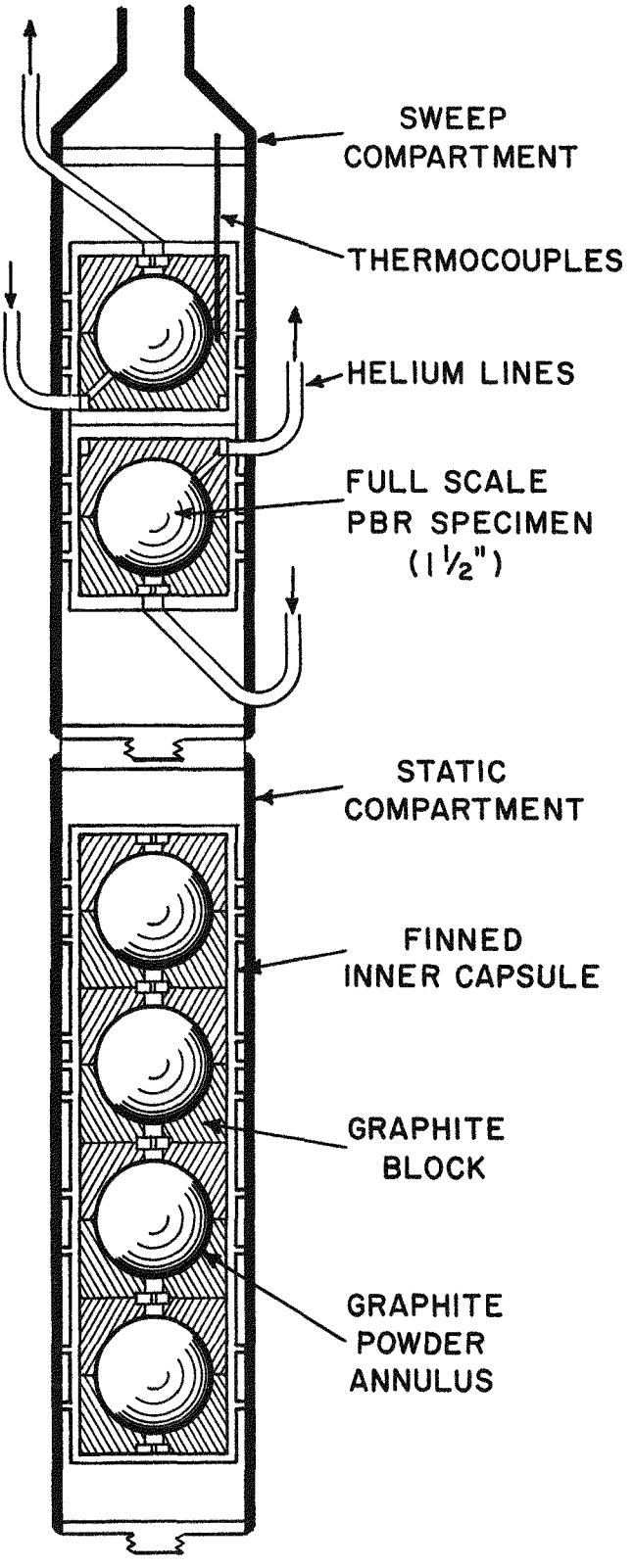

FIG. 5-2 SWEEP CAPSULE SP-5

TABLE 5-3

OPERATING CONDITIONS FOR SPECIMENS IN CAPSULE SP-5 DURING CYCLES 1 AND 2

Specimen No.	Measured Block Temp., °F		Ht. Gen. Rate, KW		Calc. Surface Temp. °F		Calc. Central Temp., °F	
	1st	2nd	1st	2nd	1st	2nd	1st	2nd
Sweep:								
FA-22(471E)	970	1090	1.3	1.5	1200	1360	1370	1550
FA-23(E8-7)	890	1010	1.4	1.6	1120	1300	1240	1440
Static:								
FA-22(470E)	-	-	1.3	1.4	1200	1360	1370	1540
FA-20(338E)	-	-	1.1	1.3	1200	1360	1280	1460
FA-23(E8-12)	-	-	0.9	1.0	1120	1300	1200	1390
FA-20(345E)	-	-	0.7	0.8	1200	1360	1250	1420

The improvement in power level from the 1st to the 2nd cycle noted in Table 5-3 was caused by a reshuffling of fuel elements in the BRR. The conditions listed for the 2nd cycle are expected to apply during the remainder of the irradiation.

A schematic diagram of the off-gas train used to measure fission product leakage rates is shown in Figure 5-3. Two independent gas trains are included. Sweep helium flow is maintained continuously throughout the irradiation. The flow is normally through a doubly-contained by-pass line directly to the final activity removal traps. Fission product concentrations in this helium stream are measured by diverting a portion of the flow through the analytical train for a period of about 2 hours. During the 1st cycle, some trap plugging caused by excessive moisture in the helium prevented sampling of the FA-23 specimen. A redesigned trap and an improved helium supply permitted normal operation during the 2nd cycle. Gross activity levels are continuously monitored by a detector mounted on the gas line.

Special underwater traps for the non-volatile daughter products of the short-lived noble fission product gases were installed as shown in Figure 5-3. These traps consist of a stainless steel container 2-1/2 in. OD by 36 in.

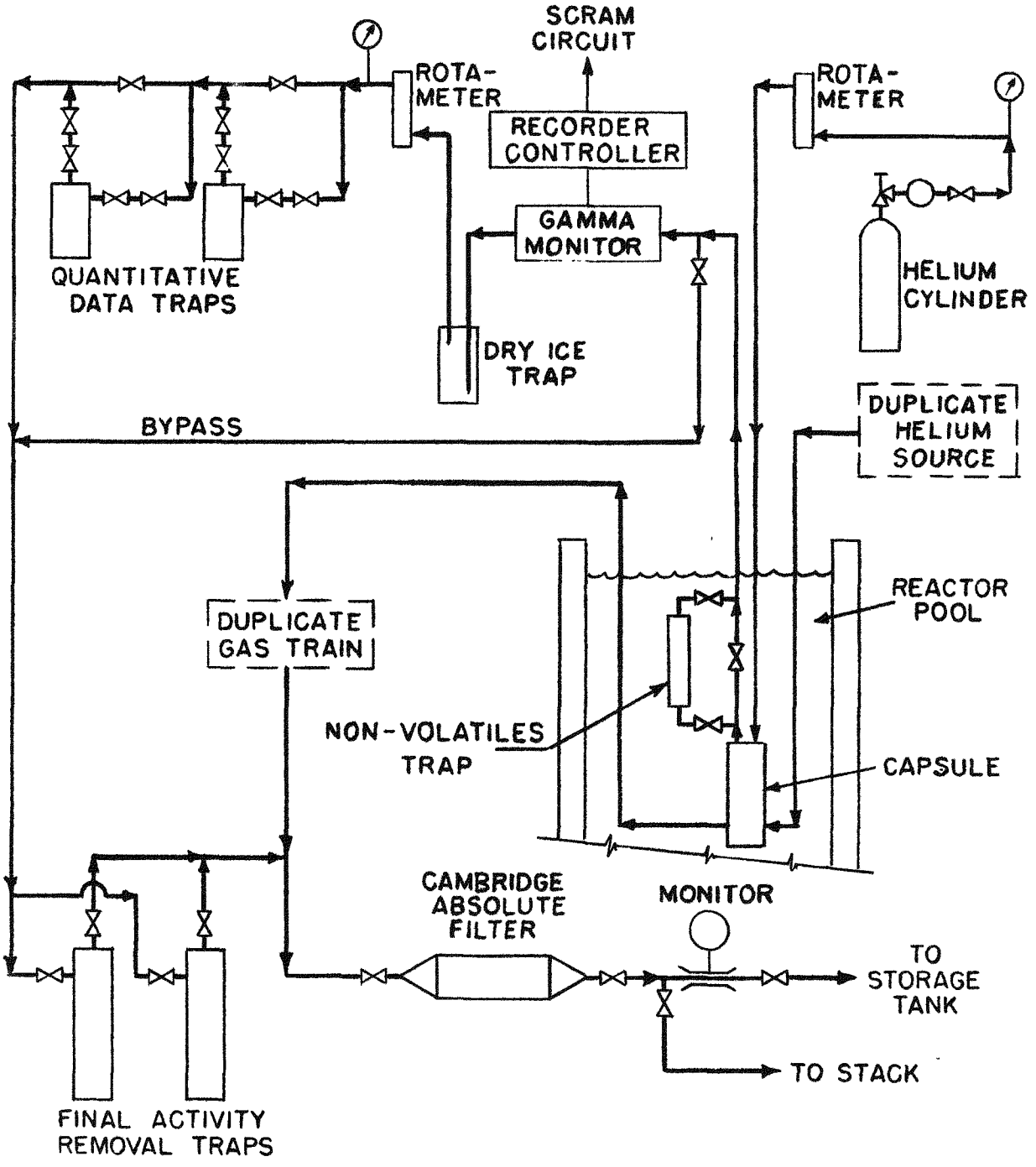

FIG. 5-3. GAS TRAIN FOR MEASURING VOLATILE FISSION PRODUCT RELEASE FROM SWEEP CAPSULE SPECIMENS

long filled with layers of stainless steel mesh. The sweep helium flow normally by-passes these traps. A sample is taken by actuating the underwater valves and diverting the full flow through the trap. Segments of the stainless steel mesh can be removed from the trap and radiochemically analyzed for such isotopes as Sr 89, Ba 140, Ce 141 and I 131.

Data obtained for the long-lived volatile fission product release is given in Section 3.1.2 for the FA-23 specimen and in Section 4.1.3 for the FA-22 specimen. It is planned to operate the first set of non-volatile traps early in the next quarter.

6.0 In-Pile Loop

The design and construction of an in-pile loop to study the behaviour of fission products escaping from a PBR fuel element was continued during this quarter under a subcontract to the Nuclear Science and Engineering Corp. The purposes of this loop are to study the equilibrium activity levels in a recycle helium stream; methods of lowering gas stream activity level; the amount, location, and nature of deposited fission products; and methods of decontaminating equipment surfaces. In addition to testing low-release PBR fuel element specimens, and uncoated specimen will be tested to simulate problems of a "dirty" primary loop.

The in-pile portion of the loop will be inserted in experimental hole W-11 of the Brookhaven Graphite Reactor with the blowers, heat exchangers, sampling stations, etc. located on the adjacent floor space. Design characteristics of the loop are as follows:

Circulating Fluid	Helium
Operating Pressure	14 psia
Flow Rate	8 scfm
Max. Helium Temp.	1250°F
Min. Helium Temp.	250°F
Max. Specimen Temp.	1800°F
Max. Specimen Power	0.25 KW

Two major variables, the system pressure and the specimen power, have been selected with a view to minimizing the cost of the loop. The use of subatmospheric pressure eliminates the need for double containment while the modest power level in the specimen will provide measurable activity yet minimize the gas flow requirements and shielding costs.

Figure 6-1 is a schematic diagram of the in-pile loop. Gas leaves the in-pile section at 1250°F and enters the shell side of a coiled tube heat exchanger where it is cooled to 550°F. The exchanger is designed for easy replacement of the tube coil so that deposition on the tube surface as a function of temperature can be studied. An intermediate Dowtherm loop, which transports heat from this exchanger to a water-cooled sink, has been included to permit adequate control of the helium outlet temperature. The helium next passes through a removable 550°F test section and a precooler to lower the temperature to 250°F which enables the use of an economical

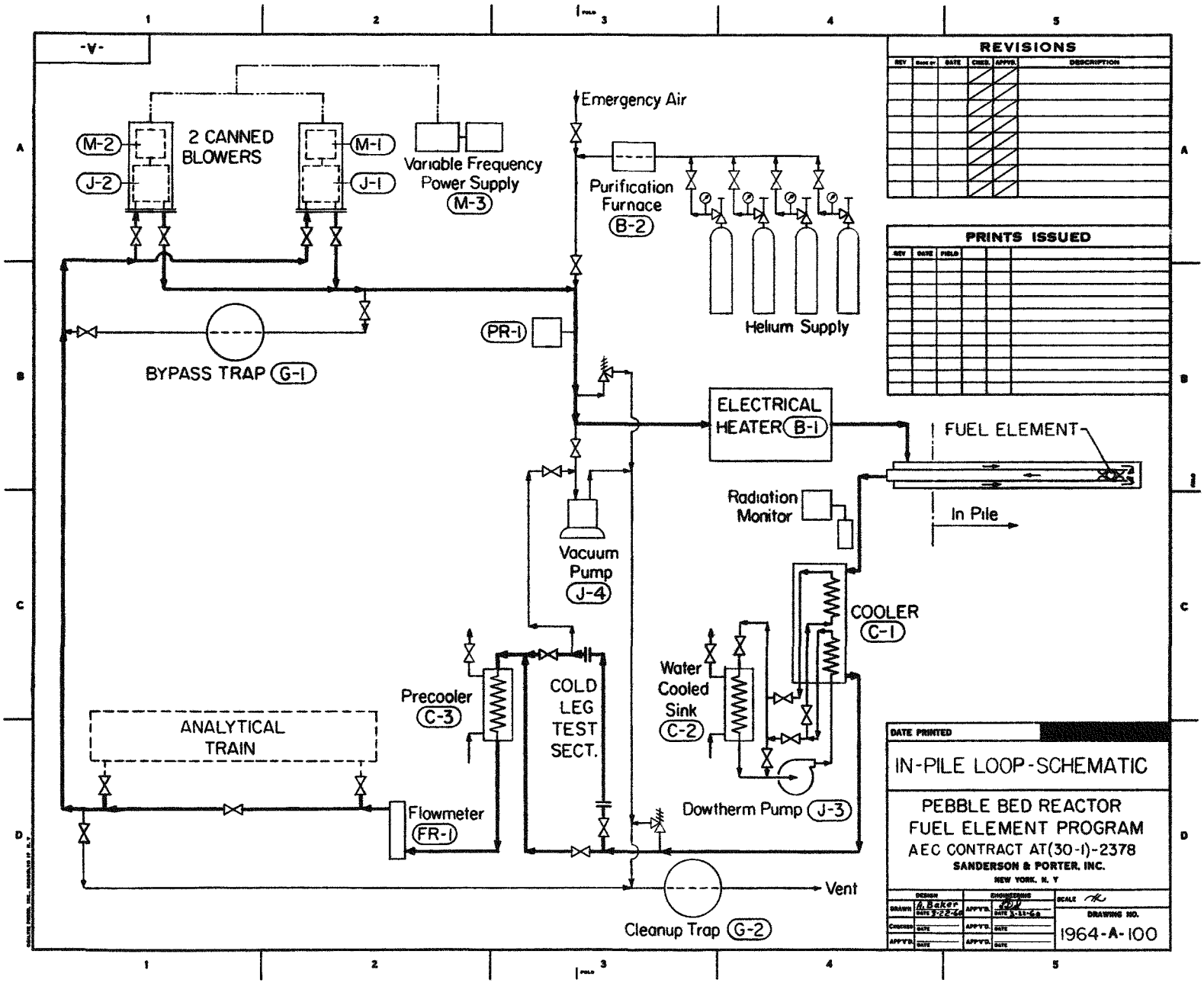

FIG. 6-1 UNCLASSIFIED

low temperature blower. Before entering the blower, provision is made for in-line or bypass operation of an analytical train which will gather data on fission product release rate and activity levels in the gas stream.

Two Dexter-Conde positive displacement blowers are provided, although only one is required for normal operation. Each blower and its drive motor are mounted in a canned enclosure to provide a zero leakage system. Flow variation is achieved by powering the drive motors from a variable frequency motor generator set. A bypass charcoal trap is provided from the blower discharge back to the blower inlet so that the effect of continuous gas decontamination can be studied. After leaving the blower, the helium temperature is raised to 1200°F by an electrical resistance heater and then enters the in-pile section.

The in-pile section is designed for accommodation in a four inch square experimental hole. Co-axial flow is used in the in-pile region, while separated pipes are possible in most of the shield plug. A flange near the point where the inlet and outlet pipes become co-axial permits removal of the test specimen and high temperature plate-out coupons. A vacuum jacket insulates the co-axial section while fibrous insulation is used for the inlet and outlet pipes. The test specimen, a fueled 1-1/2 inch graphite sphere, is surrounded with portions of dummy spheres to simulate the flow pattern in a ball bed. Fig. 6-2 is a photograph of the mock up of the test specimen holder showing the three partial spheres at each end holding the test specimen in place.

Purchase orders for all materials and equipment have been placed and most of the major equipment has been delivered. The out-of-pile system will be assembled at NSEC in three sections to permit ease of shipment to BNL. Prior to insertion in the BNL reactor, the in-pile portion of the loop will be assembled to the out-of-pile section for pre-operational testing. A special graphite sphere containing a miniature 0.25 KW electrical heater will be used to simulate nuclear heating in the fueled test specimen, thus permitting shakedown testing to be performed in the absence of radiation. Irradiation is scheduled to begin during the quarter commencing Aug. 1, 1960.

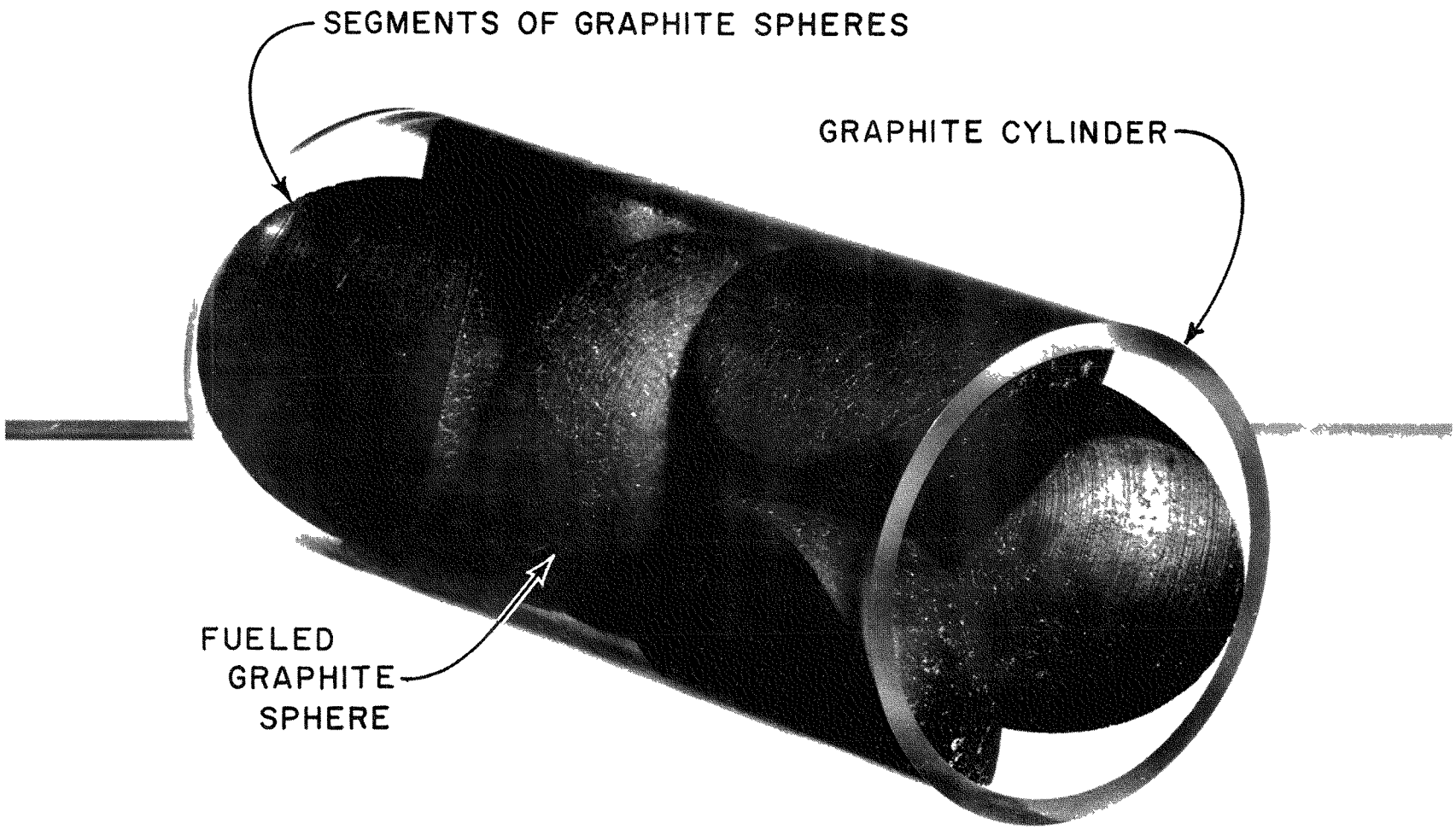

Fig. 6-2. Mockup of Test Specimen Holder for In-Pile Loop

List of References

1. NYO 8753, Vol. I; Design and Feasibility Study of a Pebble Bed Reactor-Steam Power Plant; Sanderson & Porter; May 1, 1958.

2. NYO 2373; Progress Report on the Pebble Bed Reactor Program; Sanderson & Porter; June 1, 1958 to May 31, 1959.

3. NYO 2706; Phase I Progress Report on the Fuel Element Development Program for the Pebble Bed Reactor; Sanderson & Porter; May 1 to October 31, 1959.

4. S&P 1964-14; Quarterly Progress Report on the Fuel Element Development Program for the Pebble Bed Reactor; Sanderson & Porter; November 1, 1959 to January 31, 1960.

5. NYO 9059; Thorium Oxide Infiltration of Graphite Spheres; W. E. Parker and F. Rusinko, Jr; Speer Carbon Co.; June 15, 1960.

6. Private Communication from R. Schulten, Brown-Boveri-Krupp, Mannheim, Germany.

7. Summary Report on Phase I of AT(40-1)-2560; Graphite Matrix Nuclear Fuel Elements, Vol. I; National Carbon Company; December 22, 1959.

8. AECU 4480; Symposium on High Temperature Technology; pp 108-133; W. D. Kingery.